Regular and irregular cycling near a heteroclinic network

C M Postlethwaite and J H P Dawes

DAMTP, Centre for Mathematical Sciences, Wilberforce Road, Cambridge, CB3 0WA

E-mail: `C.Postlethwaite@damtp.cam.ac.uk`

Abstract. Heteroclinic networks are invariant sets containing more than one heteroclinic cycle. Such networks can appear robustly in equivariant vector fields. Previous authors have demonstrated that trajectories near heteroclinic networks can be attracted to one of a number of simultaneously 'stable' invariant subsets of the network. None of these invariant sets are asymptotically stable, but do satisfy weaker definitions of stability. In this paper we discuss the behaviour of trajectories for one specific symmetric vector field. This vector field contains a robust heteroclinic network and nearby trajectories display a variety of interesting dynamics. In particular, trajectories are observed to settle into a pattern of excursions around different parts of the network that we call 'cycling cycles'. Cycling patterns displaying different numbers of loops around the individual component cycles can be stable for the same parameter values, as can combinations of regular and irregular cycling. Analytic results for the regular cycling behaviour agree well with numerical simulations. We show that there exist parameter values where some trajectories display irregular cycling behaviour, in the sense that the numbers of loops around individual cycles forms a bounded aperiodic infinite sequence.

1. Introduction

A heteroclinic orbit γ_1 between two equilibria ξ_1 and ξ_2 of a continuous time dynamical system $\dot{x} = f(x)$ is a trajectory $\phi_t(y)$ that is backward asymptotic to ξ_1 and forward asymptotic to ξ_2. A heteroclinic cycle is an invariant set X consisting of the union of a set of equilibria $\{\xi_1, ..., \xi_n\}$ and orbits $\{\gamma_1, ..., \gamma_n\}$, where γ_i is a heteroclinic orbit between ξ_i and ξ_{i+1}; and $\xi_{n+1} \equiv \xi_1$.

In generic dynamical systems, heteroclinic cycles are of high codimension. However, if the heteroclinic orbits lie in invariant subspaces, the cycle can be robust to perturbations of the system that preserve the invariance of these subspaces. This situation can arise if the dynamical system commutes with a group of symmetries, as is often the case in models of physical systems, or in models of population dynamics or game theory, where extinction is a preserved quantity (see the book by Hofbauer and Sigmund (1988) for examples of this).

Table 1. Classification of eigenvalues.

eigenvalue class	subspace
radial (r)	$L_j \equiv P_{j-1} \cap P_j$
contracting (c)	$P_{j-1} \ominus L_j$
expanding (e)	$P_j \ominus L_j$
transverse (t)	$(P_{j-1} + P_j)^\perp$

More technically, suppose Γ is a compact Lie group acting linearly on $\mathbb{R}^n$, and suppose $f : \mathbb{R}^n \to \mathbb{R}^n$ satisfies $f(\gamma x) = \gamma f(x) \ \forall \ \gamma \in \Gamma$: we say that f is Γ-equivariant. For $\Sigma \subset \Gamma$ a subgroup of Γ, we define the fixed point subspace

$$\text{Fix } \Sigma = \{x \in \mathbb{R}^n : \sigma x = x \ \forall \sigma \in \Sigma\}$$

Definition 1 *X is a* robust heteroclinic cycle *if for each j, $1 \leq j \leq n$ there exists a fixed point subspace, $P_j = \text{Fix } \Sigma_j$ where $\Sigma_j \subset \Gamma$ and*

(i) ξ_j is a saddle and ξ_{j+1} is a sink in P_j

(ii) there is a heteroclinic connection from ξ_j to ξ_{j+1} in P_j

(indices are to be taken mod n).

A much studied example of a robust heteroclinic cycle is that of Guckenheimer and Holmes (1988). Their equations have the symmetry group $\mathbb{Z}_3 \ltimes \mathbb{Z}_2^3$, and are motivated by the Küppers–Lortz instability in rotating Rayleigh–Bénard convection (Küppers and Lortz, 1969, Busse and Heikes, 1980). The equations admit a robust heteroclinic cycle between three symmetry related equilibria. Necessary and sufficient conditions for the cycle to be asymptotically stable can be given in terms of the eigenvalues of the linearisation of the flow near the equilibria. Many other examples of robust heteroclinic cycles, especially those related to physical problems, are given in the review article by Krupa (1997). Sottorcornola (2003) has given a complete classification of robust cycles in $\mathbb{R}^4$. Cycles are split into types A, B or C, depending on the symmetry of the fixed point subspaces P_j (this classification was first done by Chossat *et al* (1997)).

The stability result of Guckenheimer and Holmes has been generalised to higher dimensional robust cycles by Krupa and Melbourne (2002). They also generalise the classification of cycles into higher dimensions. The stability results depend on the eigenvalues of the linearisation of the vector field $f(x)$ about each equilibrium, which are classified as lying in certain subspaces as shown in table 1; where $P \ominus L$ denotes the orthogonal complement in P of the subspace L. It turns out that the radial eigenvalues play no part in the stability criteria for any of the three types of cycle. Conditions are given in Krupa and Melbourne (2002) for asymptotic stability of each type of cycle in terms of the contracting (c), expanding (e) and transverse (t) eigenvalues.

If a system contains more than one heteroclinic cycle they may be coupled together to form a heteroclinic network. Ashwin and Field (1999) provide a completely general definition of a heteroclinic network; in this paper we will only be concerned with flows

in $\mathbb{R}^n$ where each node in the network is an equilibrium of the flow (rather than e.g. a periodic orbit, a chaotic set or, indeed, another heteroclinic cycle). For our purposes, the following definition is sufficient:

Definition 2 *An invariant set N consisting of equilibria $\{\xi_1, ..., \xi_n\}$ and heteroclinic orbits $\{\gamma_1, ..., \gamma_m\}$ is a (depth 1) heteroclinic network if*

(i) (compatibility) if $x \in \gamma_i$ then $\alpha(x) = \xi_j$ and $\omega(x) = \xi_k$ for some $\xi_j, \xi_k \in N$.

(ii) (transitivity) for all ξ_i and ξ_j we can find a sequence of orbits $\{\gamma_{m_1}, ..., \gamma_{m_l}\}$ and equilibria $\{\xi_{n_1}, ..., \xi_{n_{l+1}}\}$ such that $\xi_{n_1} = \xi_i$ and $\xi_{n_{l+1}} = \xi_j$ and if $x \in \gamma_{m_k}$ then $\alpha(x) = \xi_{n_k}$ and $\omega(x) = \xi_{n_{k+1}}$.

where $\alpha(x)$ and $\omega(x)$ are the usual limit sets.

This means that if we draw the network as a directed graph between equilibria, then a path exists between any two equilibria in the network.

Within a heteroclinic network there may exist many heteroclinic cycles. A sub-cycle $X \subset N$ is an invariant set satisfying definition 1. It is clear that unless the network has only one cycle (i.e it is itself a heteroclinic cycle) then none of the sub-cycles can be asymptotically stable. This is because each sub-cycle must contain at least one equilibrium with a two-dimensional unstable manifold, (by the transitivity property *(ii)* in definition 2) so there will be points near the cycle which are contained in a heteroclinic orbit to an equilibrium not contained in the cycle. However, sub-cycles can still be strongly attracting, in the following sense.

Definition 3 (adapted from Melbourne (1991)) *An invariant set X is* essentially asymptotically stable (e.a.s.) *if there exists a set $\mathcal{A}$ such that given any real number $a \in (0, 1)$, and any neighbourhood $\mathcal{U}$ of X, there is an open neighbourhood $\mathcal{V} \subset \mathcal{U}$ of X such that:*

(i) All trajectories starting in $\mathcal{V} \setminus \mathcal{A}$ remain in $\mathcal{U}$,

(ii) All trajectories starting in $\mathcal{V} \setminus \mathcal{A}$ are asymptotic to X,

(iii) $\mu(\mathcal{V} \setminus \mathcal{A})/\mu(\mathcal{V}) > a$, where μ is Lebesgue measure.

If only (ii) and (iii) are satisfied, we say that X is essentially quasi-asymptotically stable (e.q.a.s.).

If condition *(iii)* is relaxed to $\mu(\mathcal{V} \setminus \mathcal{A}) > 0$ then the set X is a Milnor attractor (Milnor (1985)); any set which is e.a.s. is also a Milnor attractor. Melbourne (1991) describes an example of an e.a.s. heteroclinic cycle which is not part of a network, but, having positive transverse eigenvalues, cannot be asymptotically stable.

A simple example of a heteroclinic network with two sub-cycles was studied by Kirk and Silber (1994) (and also by Brannath (1994), who also considered other possible networks in $\mathbb{R}^4$). They found that it was not possible for both sub-cycles to be simultaneously e.a.s., however they could both be attracting in some sense, and the network considered as a whole could be e.a.s.. They also found that if one sub-cycle

is unstable, then 'switching' between the sub-cycles could occur. That is, a trajectory starting close to the network may make a number of excursions near to one of the cycles, and then switch to cycling near the other. In their example, with only two sub-cycles, the switching could only occur in one direction and there were no points in a neighbourhood of the cycle with ω-limit sets equal to the entire network.

Ashwin and Field (1999) considered a heteroclinic network in $\mathbb{R}^9$ with symmetry $\mathbb{Z}_2^9 \rtimes (\mathbb{Z}_3 \times \mathbb{Z}_3) \equiv (\mathbb{Z}_3 \times \mathbb{Z}_3) \wr \mathbb{Z}_2$, where $\wr$ denotes the wreath product. Essentially this is three Guckenheimer–Holmes cycles coupled together in a ring. They find that a variety of types of network may exist and develop a general method of creating networks of arbitrary depth by forming 'nested' wreath products. Ashwin and Field concentrate on the intrinsic network structure, rather than a description of the dynamics of trajectories near the network.

In this paper we consider a network constructed from a pair of Guckenheimer–Holmes cycles, coupled in a different way. We find that switching can occur between sub-cycles as in the Kirk and Silber case, but in our example this switching can happen in a cyclical manner.

This paper is organised as follows. In section 2 we define the symmetries and the specific o.d.e.s for the example system we consider and show that it contains a robust heteroclinic network. We describe the sub-cycles contained within the network and discuss their stability. In section 3 we describe the 'cycling cycles' trajectories and discuss the analytic methods used to determine the stability of the regular cycling trajectories. We also explain our numerical methods. In section 4 we show numerical results for irregular cycling and state and prove two lemmas to show that for particular parameter values there will be initial conditions for which the trajectory must display this aperiodic yet bounded (in a certain sense) behaviour. Section 5 concludes.

2. Structure and basic properties

2.1. System definition

In this section we describe the symmetries of the system of o.d.e.s, under consideration. We show that it contains a robust heteroclinic network and describe the stability of some of its sub-cycles.

The phase space we work in is $\mathbb{R}^6 = \mathbb{R}^3 \oplus \mathbb{R}^3$, denoting points as $(\boldsymbol{x}, \boldsymbol{y})$ where $\boldsymbol{x} = (x_1, x_2, x_3)$ and $\boldsymbol{y} = (y_1, y_2, y_3)$. We refer to the subspace $\{\boldsymbol{y} \equiv \boldsymbol{0}\}$ as the $\boldsymbol{x}$-subspace and $\{\boldsymbol{x} \equiv \boldsymbol{0}\}$ as the $\boldsymbol{y}$-subspace. We consider a set of equations that are equivariant under the group generated by the symmetry elements:

$$\kappa_x(\boldsymbol{x}, \boldsymbol{y}) = (\kappa\boldsymbol{x}, \boldsymbol{y})$$
$$\kappa_y(\boldsymbol{x}, \boldsymbol{y}) = (\boldsymbol{x}, \kappa\boldsymbol{y})$$
$$\rho(\boldsymbol{x}, \boldsymbol{y}) = (\sigma\boldsymbol{x}, \sigma\boldsymbol{y})$$

where $\kappa(x, y, z) = (-x, y, z)$ and $\sigma(x, y, z) = (y, z, x)$. These group elements give a reducible action of $\mathbb{Z}_3 \ltimes \mathbb{Z}_2^6$ on $\mathbb{R}^3 \oplus \mathbb{R}^3$.

The most general equivariant o.d.e.s, truncated at third order, are:

$$\dot{x}_1 = x_1(\mu + a_1 x_1^2 + a_2 x_2^2 + a_3 x_3^2 + b_1 y_1^2 + b_2 y_2^2 + b_3 y_3^2)$$
$$\dot{x}_2 = x_2(\mu + a_1 x_2^2 + a_2 x_3^2 + a_3 x_1^2 + b_1 y_2^2 + b_2 y_3^2 + b_3 y_1^2)$$
$$\dot{x}_3 = x_3(\mu + a_1 x_3^2 + a_2 x_1^2 + a_3 x_2^2 + b_1 y_3^2 + b_2 y_1^2 + b_3 y_2^2)$$
$$\dot{y}_1 = y_1(\hat{\mu} + \hat{a}_1 y_1^2 + \hat{a}_2 y_2^2 + \hat{a}_3 y_3^2 + c_1 x_1^2 + c_2 x_2^2 + c_3 x_3^2)$$
$$\dot{y}_2 = y_2(\hat{\mu} + \hat{a}_1 y_2^2 + \hat{a}_2 y_3^2 + \hat{a}_3 y_1^2 + c_1 x_2^2 + c_2 x_3^2 + c_3 x_1^2)$$
$$\dot{y}_3 = y_3(\hat{\mu} + \hat{a}_1 y_3^2 + \hat{a}_2 y_1^2 + \hat{a}_3 y_2^2 + c_1 x_3^2 + c_2 x_1^2 + c_3 x_2^2)$$

$$(1)$$

In addition we demand that both the $\boldsymbol{x}$- and $\boldsymbol{y}$-subspaces contain identical Guckenheimer–Holmes cycles which are asymptotically stable within these subspaces, implying that $\hat{a}_i = a_i$ and $\hat{\mu} = \mu$. This restriction arises in a group-theoretic way when a steady-state bifurcation problem on a rotating hexagonal superlattice is considered. The normal form for this bifurcation (truncated at third order) is exactly that given above within the subspace where the mode amplitudes are real. The additional restriction arises as a hidden symmetry of the superlattice bifurcation problem.

We refer to these two Guckenheimer–Holmes cycles as the xxx and yyy cycles respectively. For asymptotic stability, we require $c > e > 0$ where

$$c = \mu\left(-1 + a_3/a_1\right) \qquad e = \mu\left(1 - a_2/a_1\right)$$

By rescaling variables in (1), we can fix $\mu = 1$, and $a_1 = -1$.

Clearly any co-ordinate hyperplane is invariant under the flow. There are two types of axial equilibria (i.e. equilibria with maximal isotropy): those lying on the co-ordinate axes, and those with e.g., $x_1 = x_2 = x_3$, $\boldsymbol{y} = \boldsymbol{0}$. We will not discuss equilibria of this second kind in what follows. We label those equilibria on the x_i co-ordinate axes as ξ_i, and those on the y_i co-ordinate axes as η_i. The isotropy subgroup of ξ_1 is $\Sigma_{\xi_1} = \langle \rho^2 \kappa_x \rho, \rho \kappa_x \rho^2, \kappa_y, \rho^2 \kappa_y \rho, \rho \kappa_y \rho^2 \rangle$.

If all the coefficients b_j, c_j are less than -1, then the Guckenheimer–Holmes cycles are decoupled; that is, they are both asymptotically stable and there are no heteroclinic connections between equilibria contained in different cycles. Now consider increasing b_2 through -1, examining the dynamics in the $x_1 - y_2$ co-ordinate plane (figure 1). The unstable 'mixed-mode' equilibrium in the $x_1 - y_2$ plane disappears in a pitchfork bifurcation at $b_2 = -1$, and a heteroclinic orbit from η_2 to ξ_1 is created. By symmetry, heteroclinic orbits are also formed between η_3 and ξ_2, and η_1 and ξ_3. This, in itself, is not enough to create a heteroclinic network, as there are no orbits connecting any of the ξ_i equilibria to one of the η_j equilibria and so the transitivity condition is not satisfied. However, if we also increase c_2 through -1 we can form additional orbits $\xi_1 \to \eta_3$, $\xi_2 \to \eta_1$ and $\xi_3 \to \eta_2$. This creates the simplest possible heteroclinic network that can be formed by coupling two Guckenheimer–Holmes cycles in this way. (Note that if additionally, $b_1 > -1$, we have a more complicated network, with a larger number of connections between the ξ_i and η_j, but we do not consider this case here.) We then
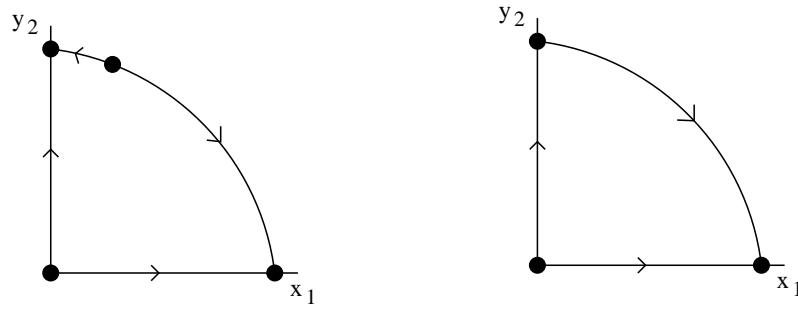
Figure 1. The left hand picture shows the $x_1 - y_2$ plane when $b_2 < -1$, and the right hand picture when $b_2 > -1$. The 'mixed-mode' equilibrium disappears in a pitchfork bifurcation, creating a heteroclinic connection.
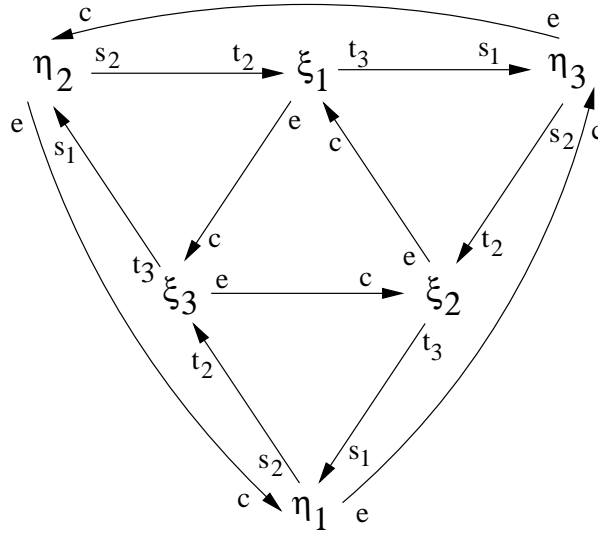

Figure 2. The figure shows a schematic illustration of the heteroclinic connections forming the network. The eigenvalues at each equilibria are labelled as expanding (e), contracting (c) or transverse (s_i, t_i) according to the classification in table 1 applied to the Guckenheimer–Holmes cycles $\xi_1 \to \xi_3 \to \xi_2$ and $\eta_1 \to \eta_3 \to \eta_2$.

rewrite the o.d.e.s (1) as:

$$\dot{x}_1 = x_1(1 - \mathbf{X}^2 + ex_2^2 - cx_3^2 - s_3y_1^2 + s_2y_2^2 - s_1y_3^2)$$
$$\dot{x}_2 = x_2(1 - \mathbf{X}^2 + ex_3^2 - cx_1^2 - s_3y_2^2 + s_2y_3^2 - s_1y_1^2)$$
$$\dot{x}_3 = x_3(1 - \mathbf{X}^2 + ex_1^2 - cx_2^2 - s_3y_3^2 + s_2y_1^2 - s_1y_2^2)$$
$$\dot{y}_1 = y_1(1 - \mathbf{X}^2 + ey_2^2 - cy_3^2 - t_1x_1^2 + t_3x_2^2 - t_2x_3^2)$$
$$\dot{y}_2 = y_2(1 - \mathbf{X}^2 + ey_3^2 - cy_1^2 - t_1x_2^2 + t_3x_3^2 - t_2x_1^2)$$
$$\dot{y}_3 = y_3(1 - \mathbf{X}^2 + ey_1^2 - cy_2^2 - t_1x_3^2 + t_3x_1^2 - t_2x_2^2)$$

(2)

where $\mathbf{X}^2 = \sum_{i=1}^{3}(x_i^2 + y_i^2)$. The network described above exists when $s_i, t_i > 0$, for all $1 \le i \le 3$. The directed graph of equilibria and the heteroclinic connections between them is shown schematically in figure 2.

This heteroclinic network comprises many new sub-cycles, all having $3n$ equilibria. As noted previously, none of these cycles can be asymptotically stable. In the next section, we look in detail at two new types of 3-cycle (cycles containing three equilibria) and discuss their stability.

2.2. Sub-cycles in the network

The simplest new sub-cycles in the heteroclinic network are 3-cycles between two ξ equilibria and one η equilibrium (or vice-versa, by symmetry). We refer to these as xxy- and yyx-cycles respectively. There are three symmetrically related copies of each type of cycle within the network. Another cycle we will encounter later is the 6-cycle between all six equilibria; this sub-cycle contains all three heteroclinic orbits $\xi_i \to \eta_{i-1}$ and all three $\eta_i \to \xi_{i-1}$.

Any four-dimensional subspace of the form $x_i = y_{i-1} = 0$ ($i - 1$ taken mod 3) contains one xxy-cycle and one yyx-cycle. This reduced system is structurally equivalent to that considered by Kirk and Silber (1994), although in the present system we have introduced several additional restrictions on the eigenvalues at different equilibria.

The stability properties of these 3-cycles could be investigated using the standard 'small-box' and Poincaré map method, as is done by Kirk and Silber (1994). An alternative method for computing necessary conditions for stability, which we demonstrate gives the same results, is to consider the length of time T_1 spent in the neighbourhood of a given equilibrium, and the length of time T_1' spent near this equilibrium (or a symmetrically related one) after one excursion around the cycle. A necessary condition for the heteroclinic cycle to be stable is $T_1'/T_1 > 1$. This is not sufficient to assert stability in any sense since it tells us nothing about the size of the basin of attraction of the sub-cycle. From the overall structure of the network we can discuss whether a given sub-cycle is asymptotically stable, e.a.s. or is only a Milnor attractor.

2.3. Necessary conditions for stability for heteroclinic cycles

In this section we illustrate the preceding statements about computation of necessary stability conditions by re-deriving conditions for two variants of the standard Guckenheimer–Holmes cycle.

We start by considering a $\mathbb{Z}_2^3$-equivariant vector field in $\mathbb{R}^3$ that has all co-ordinate hyperplanes invariant. We consider such a vector field with a robust heteroclinic cycle, (similar to the Guckenheimer–Holmes cycle, but without the $\mathbb{Z}_3$ permutation symmetry) as shown in figure 3. Label the equilibrium on the x_i axis ξ_i, as before.

Consider a trajectory starting near ξ_3 that spends a time T_3 in a small neighbourhood of ξ_3, a time T_2 near ξ_2, a time T_1 near ξ_1, and then on returning to ξ_3 spends a time T_3' near it the second time. The x_1 component decays at a rate c_3 whilst the trajectory is near ξ_3, and whilst near ξ_2 it grows at a rate e_2. We ignore the
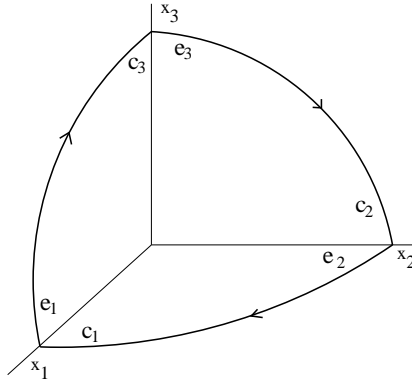
Figure 3. A $\mathbb{Z}_2^3$-equivariant vector field with a robust heteroclinic cycle in $\mathbb{R}^3$. Expanding and contracting eigenvalues at the equilibria are shown.

parts of the trajectory not near the equilibria, as the trajectory spends very little time there.

Suppose the trajectory enters a neighbourhood of ξ_3 and leaves a neighbourhood of ξ_2 when $x_1 = h \ll 1$. Then,

$$he^{-c_3 T_3 + e_2 T_2} = h$$
$$\Rightarrow T_2 = \frac{c_3}{e_2} T_3$$

similarly we find

$$T_1 = \frac{c_2}{e_1} T_2, \qquad T_3' = \frac{c_1}{e_3} T_1, \qquad \Rightarrow \frac{T_3'}{T_3} = \frac{c_1 c_2 c_3}{e_1 e_2 e_3}$$

and since there are no transverse directions, the cycle is asymptotically stable if $\prod_{i=1}^{3} c_i > \prod_{i=1}^{3} e_i$, which is the condition given by Krupa and Melbourne (1995) for such a cycle.

Now, assuming that this condition holds, consider perturbations in a direction transverse to the cycle. That is, embed the cycle in $\mathbb{R}^4$, so that at each equilibrium ξ_i there is now an additional eigenvalue t_i in the (transverse) x_4 direction. Suppose a trajectory has initial condition $x_4 = h \ll 1$, and so in a neighbourhood of ξ_i, $x_4 \sim e^{t_i T}$. Again we ignore the parts of the trajectory away from the equilibria. In fact, we consider three such trajectories, one starting near each of the ξ_i equilibria, and compare the magnitude of the x_4 co-ordinate after each trajectory has completed one full cycle. For the trajectory starting near the equilibrium ξ_i, we find $x_4 = he^{\nu_i T_i}$, where

$$\nu_1 = t_1 + t_3 \frac{c_1}{e_3} + t_2 \frac{c_1 c_3}{e_2 e_3}$$
$$\nu_2 = t_2 + t_1 \frac{c_2}{e_1} + t_3 \frac{c_1 c_2}{e_1 e_3}$$
$$\nu_3 = t_3 + t_2 \frac{c_3}{e_2} + t_1 \frac{c_2 c_3}{e_1 e_2}$$

For the cycle to be stable in any sense we require the x_4 co-ordinate to decay; hence we require $\nu_i < 0$ for all i. These conditions are the same as those derived by Kirk and
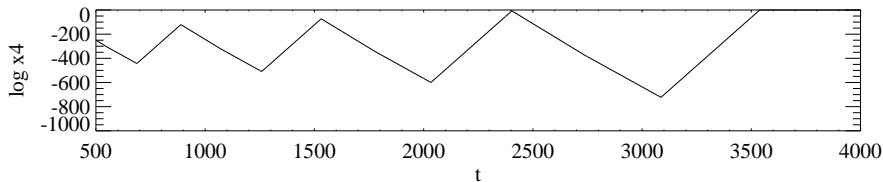
Figure 4. The logarithm of a component x_4 transverse to a 3-cycle, plotted against time. Although the minimum value over each full cycle decreases, the maximum value over a cycle increases; eventually x_4 is no longer small and so the 3-cycle is unstable.

Silber (1994) for each of their 3-cycles. Asymptotic stability requires all $t_i < 0$. Three conditions are required because there is no symmetry and the behaviour of trajectories near heteroclinic cycles is not ergodic, meaning that long-time averages cannot be taken. An example of a time series from such a trajectory is shown in figure 4. Notice that although the minimum value of $\log x_4$ over each cycle decreases, the maximum value increases, so if we were to take an 'average' of the change in x_4 over one cycle, the result would depend on where we started our average.

If $t_1 > 0$ then the cycle cannot be asymptotically stable. It could, however, be essentially asymptotically stable, depending on the shape of the domains of attraction local to each equilibrium. The shapes of these domains can be calculated using the standard box and map method, as done by Kirk and Silber (1994).

Clearly, it is possible to do similar, albeit more complicated, calculations for cycles between four, or more, equilibria, and hence reproduce the results given in Krupa and Melbourne (2002).

2.4. Stability of xxy- and yyx-cycles

We now apply the method of the previous section to the xxy- and yyx-cycles within the heteroclinic network to see in what sense either or both types of sub-cycle can be stable. Since it is the behaviour of perturbations in directions transverse to a sub-cycle that gives rise to the different kinds of stability, we assume that both cycles are stable within the 3-dimensional subspaces in which they lie. This subspace stability condition is the same for both cycles, namely $\delta^\star > 1$ where

$$\delta^\star = \frac{cs_1t_2}{es_2t_3} \tag{3}$$

Since both types of sub-cycle (xxy and yyx) have three transverse directions, there will be a total of nine conditions involved in determining the stability of each type of cycle: three conditions for each transverse direction. For simplicity, we first concentrate on the yyx-cycle $\eta_3 - \eta_2 - \xi_1$. The transverse directions at each of the equilibria are x_2, y_1 and x_3. Straightforward calculations using the methods of the previous section give the nine conditions:

$$\alpha_1, \alpha_2, \alpha_3 > 0 \qquad \beta_1, \beta_2, \beta_3 > 0 \qquad \gamma_1, \gamma_2, \gamma_3 > 0 \tag{4}$$

where

$$\alpha_1 = \frac{c}{t_3} - \frac{s_2}{e}\hat{\delta}_x + \frac{s_3}{s_2}\hat{\delta}_x\delta_3 \qquad \beta_1 = -\frac{e}{t_3} + \frac{s_3}{e}\hat{\delta}_x + \frac{s_1}{s_2}\hat{\delta}_x\delta_3 \qquad \gamma_1 = \frac{t_1}{t_3} + \frac{c}{e}\hat{\delta}_x - \frac{e}{s_2}\hat{\delta}_x\delta_3$$

$$\alpha_2 = \frac{s_3}{s_2} + \frac{c}{t_3}\delta_2 - \frac{s_2}{e}\delta_2\hat{\delta}_x \qquad \beta_2 = \frac{s_1}{s_2} - \frac{e}{t_3}\delta_2 + \frac{s_3}{e}\delta_2\hat{\delta}_x \qquad \gamma_2 = -\frac{e}{s_2} + \frac{t_1}{t_3}\delta_2 + \frac{c}{e}\delta_2\hat{\delta}_x$$

$$\alpha_3 = -\frac{s_2}{e} + \frac{s_3}{s_2}\delta_3 + \frac{c}{t_3}\delta_2\delta_3 \qquad \beta_3 = \frac{s_3}{e} + \frac{s_1}{s_2}\delta_3 - \frac{e}{t_3}\delta_2\delta_3 \qquad \gamma_3 = \frac{c}{e} - \frac{e}{s_2}\delta_3 + \frac{t_1}{t_3}\delta_2\delta_3$$

with

$$\hat{\delta}_x = \frac{t_2}{t_3} \qquad \delta_2 = \frac{c}{s_2} \qquad \delta_3 = \frac{s_1}{e}$$

where the α_i control the growth of the x_2 component, the β_i control the growth of the x_3 component, and the γ_i control the y_1 component. Simple algebraic manipulations (detailed in Appendix A) show that

$$\alpha_2 > 0 \Rightarrow \alpha_1, \alpha_3 > 0$$
$$\beta_3 > 0 \Rightarrow \beta_1, \beta_2 > 0$$
$$\gamma_1 > 0 \Rightarrow \gamma_2, \gamma_3 > 0$$

and so, of the nine conditions, these three are in fact sufficient. This is an artifact of there being only one positive transverse eigenvalue at each equilibrium. If any of the nine conditions are broken, the cycle will be unstable to perturbations in the corresponding transverse direction, and hence the basin of attraction of the cycle will have measure zero.

Similar conditions can be derived for the xxy-cycle; the details of these can be found in Appendix A.

It is possible to find parameters such that all the conditions (4) are satisfied and also all the corresponding ones for the xxy-cycle; hence for this combination of parameters, both cycles can be simultaneously attracting. However, neither type of cycle can ever be e.a.s.. To see this, consider for example the yyx-cycle $\eta_3 - \eta_2 - \xi_1$. For a trajectory to be attracted to this cycle we require that it leaves the neighbourhood of η_3 in the y_2 direction rather than in the x_2 direction. By considering the travel times from the plane $x_1 = h$ to the planes $y_2 = h$ and $x_2 = h$ we find that a trajectory starting at a point $x_1 = h$, $y_2 = \tilde{y}_2$, $x_2 = \tilde{x}_2$ follows the cycle if $\tilde{y}_2 > h_1\tilde{x}_2^{s_2/e}$ for some constant h_1. Similarly, trajectories starting from $x_2 = h$, $x_1 = \tilde{x}_1$, $y_1 = \tilde{y}_1$ near η_2 remain close to the cycle if $\tilde{x}_1 > h_2\tilde{y}_1^{e/s_2}$ for some constant h_2. Ignoring the 'resonant' case $s_2 = e$ it is clear that one of these domains of attraction is cusp-shaped and so has smaller and smaller measure relative to that of neighbourhoods of the connecting orbit. Hence the cycle cannot be e.a.s.. We find that the 'best' we can do in terms of stability is that each cycle attracts an 'essentially full' neighbourhood of points near two out of the three connecting orbits in the cycle. The network as a whole can be e.a.s., as essentially full neighbourhoods of all connections, (and so, of the entire network) are attracted to some cycle, which is a subset of the network. In this case, points in such a neighbourhood will have an ω-limit set equal to one heteroclinic sub-cycle, and not the whole network.

More interesting behaviour occurs when one or more of the cycles is unstable in a transverse direction. We will describe these phenomena in the next sections.

2.5. Essentially quasi-asymptotically stable cycles

As noted above, neither the xxy- or yyx-cycle can be e.a.s.. However, if one type of cycle is unstable in one or more transverse directions that the stability of the other type of cycle can be enhanced, and the cycle can be essentially quasi-asymptotically stable. (This phenomenon was noted by Kirk and Silber (1994), and they called it 'e.a.s. in spirit'.)

We give an example to demonstrate this. We find parameter values so that the yyx-cycle $\eta_3 - \eta_2 - \xi_1$ is unstable in the x_2 direction, and the xxy-cycles are stable in all transverse directions. Moreover, we can find parameter values so that essentially all initial conditions near the connections $\eta_3 \to \xi_2$ and $\xi_2 \to \xi_1$ are asymptotic to the $\xi_2 - \xi_1 - \eta_3$ cycle. 'Essentially all' trajectories near the $\xi_1 \to \eta_3$ connection will initially move around the $\eta_3 - \eta_2 - \xi_1$ cycle, but, since perturbations to this cycle in the x_2 direction will grow, the trajectory will eventually switch onto the $\xi_2 - \xi_1 - \eta_3$ cycle. As a result, the $\xi_2 - \xi_1 - \eta_3$ cycle is essentially quasi-asymptotically stable.

3. Cycling cycles: regular cycling

We now focus in detail on a particular kind of behaviour that can occur when both the xxy- and yyx-cycles are unstable in exactly one transverse direction. Transverse instability implies that nearby trajectories cannot be asymptotically attracted to just one sub-cycle, but always eventually switch onto the next cycle in the sequence. We will focus on the case

$$\alpha_2, \tilde{\beta}_1 < 0 \qquad \beta_3, \gamma_1, \tilde{\alpha}_3, \tilde{\gamma}_2 > 0$$

This means the $\eta_3 - \eta_2 - \xi_1$ cycle is unstable in only the x_2 direction, and the $\xi_2 - \xi_1 - \eta_3$ cycle is unstable in only the y_1 direction. Figures 5 and 6 show numerical data and a schematic illustration of such a trajectory. We can see the cycle switching from the $\xi_2 - \xi_1 - \eta_3$ cycle to the $\eta_1 - \eta_3 - \xi_2$ cycle and then to the $\xi_3 - \xi_2 - \eta_1$ cycle.

To simplify the analysis in this section we introduce an extra symmetry element γ which acts on $\mathbb{R}^6$ as follows:

$$\gamma(\boldsymbol{x}, \boldsymbol{y}) = (\sigma^2 \boldsymbol{y}, \sigma^2 \boldsymbol{x})$$

so $\gamma^2(\boldsymbol{x}, \boldsymbol{y}) = \rho(\boldsymbol{x}, \boldsymbol{y})$. The symmetry group now acting (irreducibly) on $\mathbb{R}^6$ is $\mathbb{Z}_6 \ltimes \mathbb{Z}_2^6$. Symmetry forces $s_1 = t_2$, $s_2 = t_3$ and $s_3 = t_1$, implying that $\alpha_2 = \tilde{\beta}_1$. The network now contains six symmetric copies of the xxy-cycle because the xxy- and yyx-cycles are now symmetry related.

We are particularly interested in describing the number of loops that trajectories make around each sub-cycle; for some parameter values this is constant, and we call the resulting behaviour 'regular cycling'. In section 4 we describe 'irregular cycling'
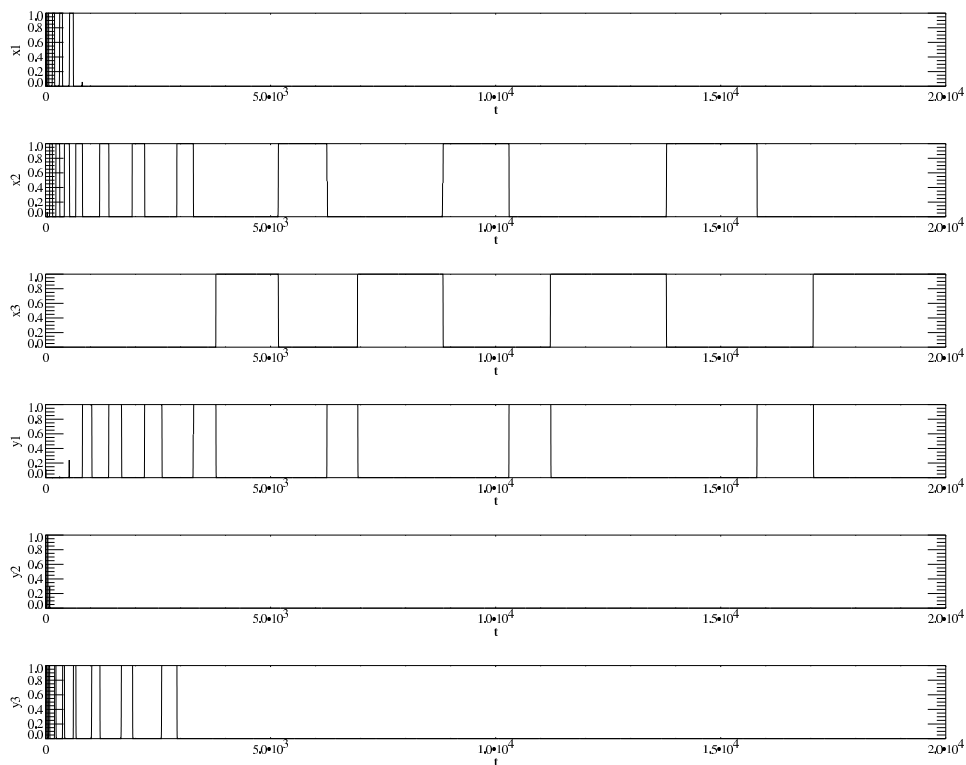
Figure 5. Numerical data from integration of equations (2), showing cycling cycles. The cycles are visited in the order $\xi_2 - \xi_1 - \eta_3$, $\eta_1 - \eta_3 - \xi_2$, $\xi_3 - \xi_2 - \eta_1$, see also figure 6. Parameter values are $c = 1$, $e = 0.5$, $s_1 = 1.4$, $s_2 = 1.6$, $s_3 = 1.1$, $t_1 = 0.9$, $t_2 = 0.7$, $t_3 = 0.9$, implying $\alpha_2 = -0.17$ and $\tilde{\beta}_1 = -0.056$.
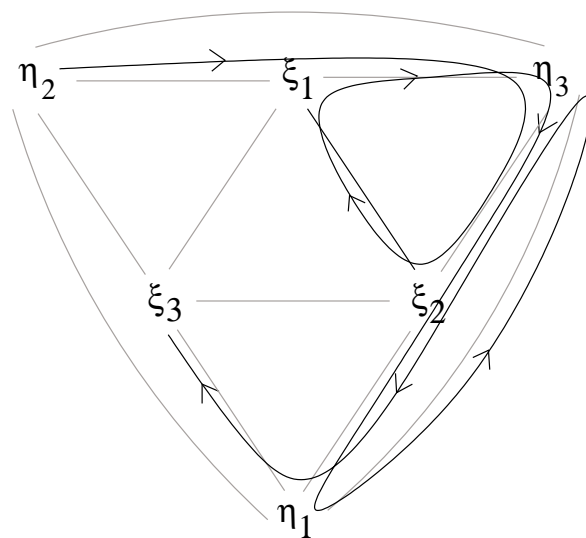

Figure 6. Schematic diagram of a cycling cycles trajectory when $\alpha_2, \tilde{\beta}_1 < 0$; compare with figure 5.

behaviour that also exists. First we briefly discuss a couple of points that help improve the speed of our numerical integrations over these extremely long integration times without losing accuracy.

3.1. Numerical methods

O.d.e.s are in general fairly simple to solve numerically, and we give a brief description here of the methods used and a few alterations made to a standard o.d.e. solver to increase the efficiency of integration for our particular system. In all the numerical simulations we have set $c = 1$ and $e = 0.5$.

The basis of the code is a standard 4th order Runge-Kutta (RK4) integrator. The trajectories we are interested in are those lying close to the heteroclinic connections, and points on these trajectories will routinely have components which become very small, as the trajectory approaches the invariant co-ordinate planes in which the connections lie. To minimise the errors which occur when computing small quantities, we apply the transformation $X_i = \log(x_i)$, $Y_i = \log(y_i)$ to (2), and integrate the equations in the form

$$\dot{X}_1 = (1 - \mathbf{X}^2 + e \exp 2X_2 - c \exp 2X_3 - s_3 \exp 2Y_1 + s_2 \exp 2Y_2 - s_1 \exp 2Y_3)$$

etc. These equations are valid in the interior of $\mathbb{R}_+^6$, which is invariant under the flow, and we restrict our attention to this region. To prevent floating underflow errors, we approximate $\exp(X)$ by 0 when $X < -300$; the error incurred here is extremely small.

The second alteration we make is applied when the trajectory is in the neighbourhood of an equilibrium. Here the flow can be very well approximated by its linearisation about the equilibrium and hence can be integrated analytically. This is implemented by the following algorithm:

- Count the number of (log) co-ordinates with value less than $-H$, for some fixed threshold (box size) $e^{-H} \ll 1$.

- If this equals five, check that the sixth co-ordinate is close to 1; this identifies which equilibrium the trajectory is near.

- Using the linearised flow around the equilibrium, calculate the time until one of the (log) co-ordinates has increased to be equal to $-H$.

- Calculate the value of all the co-ordinates at this future time using the linearised flow.

- Continue with standard RK4 away from the equilibrium, until five co-ordinates are again less than $-H$.

The times spent near successive equilibria will increase approximately geometrically in any stable heteroclinic cycle or network, and so this method massively reduces the computational time required.

The code has been checked against a standard RK4 routine for the original equations; they agree to approximately 8 significant figures. In further numerical checks, the time-step in the RK4 part of the code has been varied from $dt = 0.001$ to 0.01, and

the box size e^H has been varied from e^{-1000} to e^{-50}. Values of $dt = 0.005$ and $H = -100$ were chosen for the results presented here.

3.2. Analytic calculations

Many numerical simulations show the trajectory quickly settling to a state in which it performs a constant number of loops n around each sub-cycle. In this section we shall look at this phenomenon analytically. Note that the case $n = 0$ corresponds to the 6-cycle mentioned in section 2.2.

For a fixed n, we derive a recurrence relation for the ratio $r_i = \mathcal{T}_i/\mathcal{T}_{i-1}$ where $\mathcal{T}_i$ is the length of time spent near the ith cycle. When the number of loops becomes constant, numerical simulations indicate that r_i also converges to a constant value. The order in which the sub-cycles are visited is unique, as for each sub-cycle there is only one unstable transverse direction. For cycling trajectories we calculate the growth or decay of individual co-ordinates in terms of the times spent near each equilibrium. This allows us to produce an expression for $\mathcal{T}_i$ in terms of $\mathcal{T}_{i-1}, ..., \mathcal{T}_{i-4}$ and hence find a recurrence relation for the r_i.

Consider a trajectory starting near η_3, that initially loops n_0 times around the $\eta_3 - \xi_2 - \xi_1$ cycle. The growth or decay of the x_1 co-ordinate of the trajectory over four subsequent sub-cycles is shown in table 2, where $T_0, ..., T_4$ are unknowns and

$$\Delta_n = \frac{\delta^{\star n} - 1}{\delta^\star - 1}, \qquad \nu = \frac{s_1}{e}\left(1 + \frac{s_1}{s_2} + \frac{cs_1}{s_2^2}\right) \tag{5}$$

and $\delta^\star$ is defined in (3); recall that $t_1 = s_3$, $t_2 = s_1$ and $t_3 = s_2$.

We assume that the magnitude of the x_1 component is the same when the trajectory last enters the neighbourhood of η_3 on the $\xi_2 - \xi_1 - \eta_3$ cycle (that is, the first equilibrium which is visited after the last visit to ξ_1) and when it leaves a neighbourhood of the last equilibrium before it returns to ξ_1 (η_2 in the $\xi_1 - \xi_3 - \eta_2$ cycle, having just switched from the $\eta_2 - \eta_1 - \xi_3$ cycle), i.e. exactly as in the 'small box' approach. This implies that the overall growth factor for x_1 must be unity, i.e. the sum of all the terms in the right hand column of table 2 must be zero:

$$s_2 T_4 = (s_1 \alpha_3 \Delta_{n_3} + c)T_3 + (s_1 \gamma_3 \Delta_{n_2} + s_3)T_2 + (s_1 \beta_3 \Delta_{n_1} - e)T_1 + s_1 \delta^{\star n_0} T_0$$

Since the sub-cycles are symmetrically related we continue in this manner and find inductively that

$$T_i = A_1(n_{i-1})T_{i-1} + A_2(n_{i-2})T_{i-2} + A_3(n_{i-3})T_{i-3} + A_4(n_{i-4})T_{i-4} \tag{6}$$

where

$$\begin{aligned}
A_1(n) &= \frac{s_1}{s_2}\alpha_3\Delta_n + \frac{c}{s_2} \\
A_2(n) &= \frac{s_1}{s_2}\gamma_3\Delta_n + \frac{s_3}{s_2} \\
A_3(n) &= \frac{s_1}{s_2}\beta_3\Delta_n - \frac{e}{s_2} \\
A_4(n) &= \frac{s_1}{s_2}\delta^{\star n}
\end{aligned} \tag{7}$$

Table 2. This table shows the time spent near equilibria for cycling trajectories and the corresponding growth and decay of the x_1 co-ordinate. Recall that $\delta^\star = cs_1^2/es_2^2$.

cycle	equilibrium	time	growth or decay factor of x_1
0	η_3 ξ_2 ξ_1 η_3 $\Big\}$ n_0 times	T_0 $\frac{s_1}{e}T_0$ $\frac{s_1^2}{es_2}T_0$ $\delta^\star T_0$ $\Big\}$ $\Delta_{n_0}\nu T_0$	 $-s_1\delta^{\star n_0}T_0$
1	ξ_2 η_1 η_3 ξ_2 $\Big\}$ n_1 times	T_1 $\frac{s_1}{e}T_1$ $\frac{s_1^2}{es_2}T_1$ $\delta^\star T_1$ $\Big\}$ $\Delta_{n_1}\nu T_1$	eT_1 $-s_3\frac{s_1T_1}{e}$ $-s_1\frac{s_1^2T_1}{es_2}$ $e\delta^\star T_1$ $\Big\}$ $-s_1\beta_3\Delta_{n_1}T_1$
2	η_1 ξ_3 ξ_2 η_1 $\Big\}$ n_2 times	T_2 $\frac{s_1}{e}T_2$ $\frac{s_1^2}{es_2}T_2$ $\delta^\star T_2$ $\Big\}$ $\Delta_{n_2}\nu T_2$	$-s_3T_2$ $-c\frac{s_1T_2}{e}$ $s_2\frac{s_1^2T_2}{es_2}$ $-s_3\delta^\star T_2$ $\Big\}$ $-s_1\gamma_3\Delta_{n_2}T_2$
3	ξ_3 η_2 η_1 ξ_3 $\Big\}$ n_3 times	T_3 $\frac{s_1}{e}T_3$ $\frac{s_1^2}{es_2}T_3$ $\delta^\star T_3$ $\Big\}$ $\Delta_{n_3}\nu T_3$	$-cT_3$ $s_2\frac{s_1T_3}{e}$ $-s_3\frac{s_1^2T_3}{es_2}$ $-c\delta^\star T_3$ $\Big\}$ $-s_1\alpha_3\Delta_{n_3}T_3$
4	η_2	T_4	s_2T_4

and Δ_n is defined in (5). Note that A_4 is always positive, as is A_2, since $\gamma_1 > 0$ (assumed at the beginning of section 3) implies $\gamma_3 > 0$, using results from Appendix A. A_3 is positive for sufficiently large n since we are assuming $\beta_3 > 0$. The sign of A_1 for large n is equal to the sign of α_3 and we have so far made no assumptions about this. We define the length of time spent on each cycle to be $\mathcal{T}_i = T_i(\Delta_{n_i}\nu + 1)$, so the $\mathcal{T}_i$ also satisfy the linear recurrence relation (6). In general we have no further information about the sequence $\{n_i\}$ and it is not clear how to proceed. As a first step we consider the constant n case, setting $n_i = n$ for all i. With this simplification, we consider solutions of the recurrence relation (6) in the next section.

3.2.1. Analysis of the recurrence relation In the case $n_i = n$ for all i, equation (6) has a general solution of the form

$$T_i = a_1\rho_1^i + a_2\rho_2^i + a_3\rho_3^i + a_4\rho_4^i$$

where $a_1, ..., a_4$ are constants and $\rho_1, ..., \rho_4$ are the solutions of

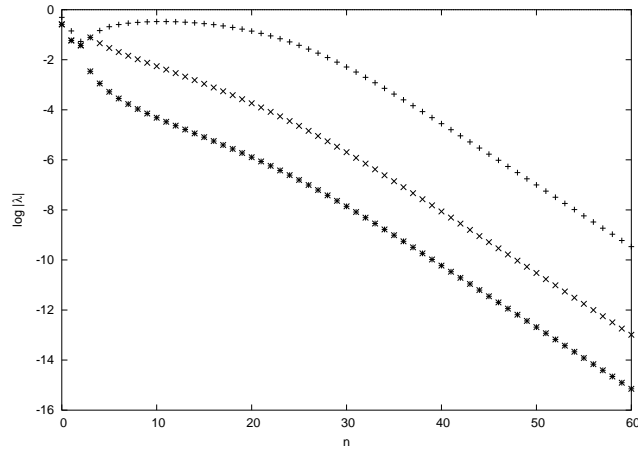$$\rho^4 - A_1\rho^3 - A_2\rho^2 - A_3\rho - A_4 = 0 \tag{8}$$

Figure 7. The graph shows $\log|\lambda|$ for the three Floquet multipliers λ of the positive fixed point of the map (9) against n, for the parameters $s_1 = 1.0$, $s_2 = 1.25$, $s_3 = 0.8$. Here $\alpha_3 > 0$, and all fixed points are stable.

Assume that ρ_1 is the root of (8) with magnitude strictly greater than $\rho_2, ..., \rho_4$, then $\left|\frac{T_i - a_1 \rho_1^i}{a_1 \rho_1^i}\right| \to 0$ as $i \to \infty$. Hence $r_i \equiv \frac{T_i}{T_{i-1}} \to \rho_1$ as $i \to \infty$ and the only stable fixed point of the related recurrence relation for r_i

$$r_i = A_1(n) + \frac{A_2(n)}{r_{i-1}} + \frac{A_3(n)}{r_{i-1}r_{i-2}} + \frac{A_4(n)}{r_{i-1}r_{i-2}r_{i-3}} \tag{9}$$

is $r_i = \rho_1$; all other fixed points of this recurrence relation will be unstable. In consequence, if $\rho_1 < 1$ then the positive, and therefore relevant, solutions for r_i will be unstable.

When n becomes large, the coefficients $A_1, ..., A_4$ all scale as $\delta^{\star n}$. In the limit of large n, it is clear to see that there is one root of (8) where $\rho \sim A_1(n)$ and three more where $\rho \sim 1$. If $A_1(n) > 0$ then the root $\rho \sim A_1(n)$ is both stable, since it is the root with the largest magnitude, and meaningful in the context of $r > 0$ being a ratio of cycle times. If $A_1(n) < 0$ for large n, then the root $\rho \sim A_1(n)$ has no proper meaning in this context and, moreover, its stability guarantees that any other positive root will be unstable as a fixed point of (9).

From (7), for large n the sign of A_1 is equal to the sign of α_3. If $\alpha_3 > 0$, we expect that stable regular cycling cycles trajectories are possible for all sufficiently large n. If, on the other hand, $\alpha_3 < 0$, then we would expect only a limited number of stable cycling cycle trajectories to be possible, all for small n (it is this case which causes the irregular cycling which we will consider in section 4).

For a particular set of parameter values, we can locate the fixed points of (9) and compute their stability for any n. Figures 7 and 8 show $\log|\lambda_j|$ against n, where the λ_j are the Floquet multipliers of the positive fixed point of (9). Figure 7 illustrates the case $\alpha_3 > 0$, and all fixed points are stable. In figure 8 we have $\alpha_3 < 0$, and there are stable fixed points for $0 \le n \le 7$, but all large n fixed points are unstable. This suggests that we should be able to find initial conditions for trajectories which undergo regular
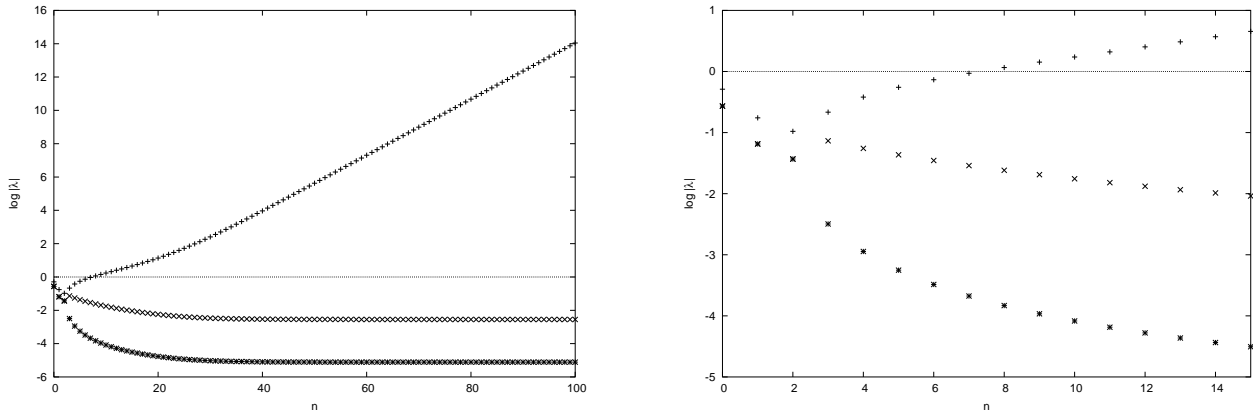
Figure 8. The graphs show $\log|\lambda|$ for the three Floquet multipliers λ of the positive fixed point of the map (9) against n, for parameter values $s_1 = 1.0, s_2 = 1.3, s_3 = 0.8$. The right hand graph is a close up of the graph for $0 \leq n \leq 15$. If any of the three plotted points are positive, the fixed point is unstable. This example has $\alpha_3 < 0$, so all large n fixed points are unstable.

Table 3. Comparison of limiting ratios of time spent on consecutive cycles for various n, computed analytically and from numerical integration. Parameter values are $s_1 = 1.0, s_2 = 1.3, s_3 = 0.8$, as for figure 8.

n	0	2	4	5
Analytic result, (9)	1.336540953711	2.66521546892	3.5205959481	3.9102073410
Numerical integration	1.336540953725	2.66521546933	3.5205959475	3.910207

cycling with n loops around each sub-cycle, only for n in the range $0 \leq n \leq 7$. We do not, however, know the sizes of the basins of attraction for different n.

3.3. Numerical results and comparison with analytic results

For the parameter values $s_1 = 1.0, s_2 = 1.3, s_3 = 0.8$, we were able to find initial conditions for regular cycling cycles trajectories with n equal to 0, 2, 4 and 5. Table 3 shows the ratios as computed analytically and the limit found by numerical computation. The agreement is excellent. For these particular values, convergence to the final n occurred very rapidly, within 10 cycles at most. However, this is not always the case, and for some initial conditions we observe irregular transients: figure 9 shows the number of loops around each sub-cycle for three different initial conditions for the slightly different parameters $s_1 = 1.1, s_2 = 1.5, s_3 = 0.8$, and the corresponding Floquet multipliers for each n; we see that $n = 0, 1, 2$ are stable whilst all $n > 2$ are unstable. Two of the three trajectories shown eventually converge to $n = 2$; the third does not settle down in the length of time the integration could be carried out for; this was approximately $t = 10^{39}$.
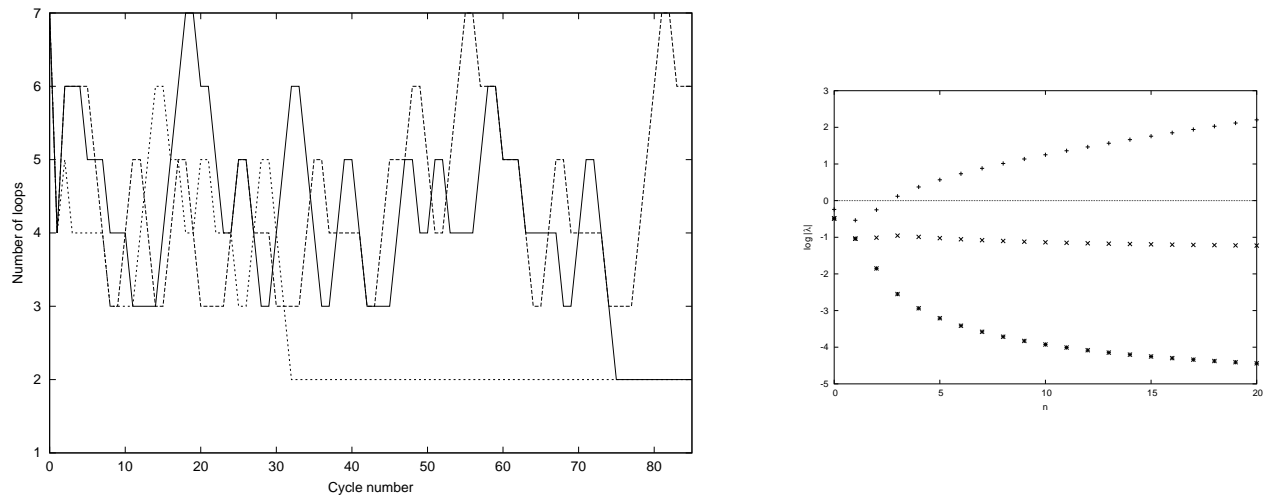
Figure 9. The left hand graph shows the number of loops around sub-cycles, for three trajectories with very similar initial conditions. Two of the trajectories eventually converge on $n = 2$, but the third does not.log $|\lambda|$ for the three Floquet multipliers λ of the positive fixed point of the map (9) are shown in the right hand graph. Notice that for $n \geq 3$ the fixed point is unstable. Parameter values are $s_1 = 1.1, s_2 = 1.5, s_3 = 0.8$.
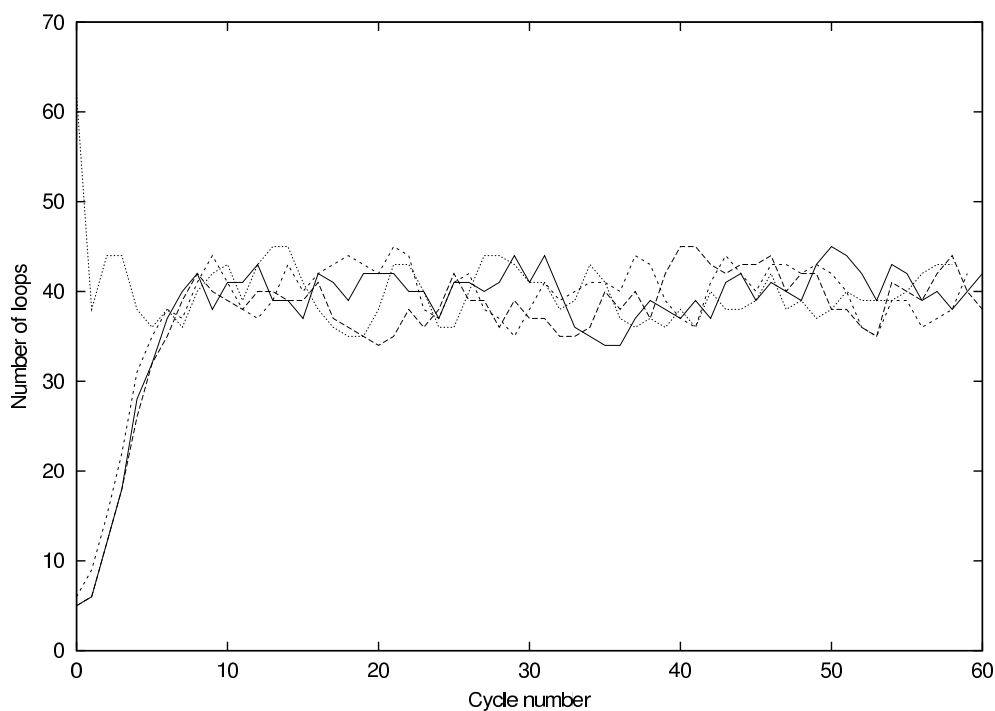

Figure 10. The graph shows the number of loops around a sub-cycle versus the number of the sub-cycle in the sequence, for three trajectories with very similar initial conditions, and a fourth with different initial conditions, such that the number of loops around the first cycle is large. Parameter values are $s_1 = 1.0, s_2 = 1.4, s_3 = 0.8$. Note that the lines on the graph are only for clarity, and it is the points at each cycle number which are important.
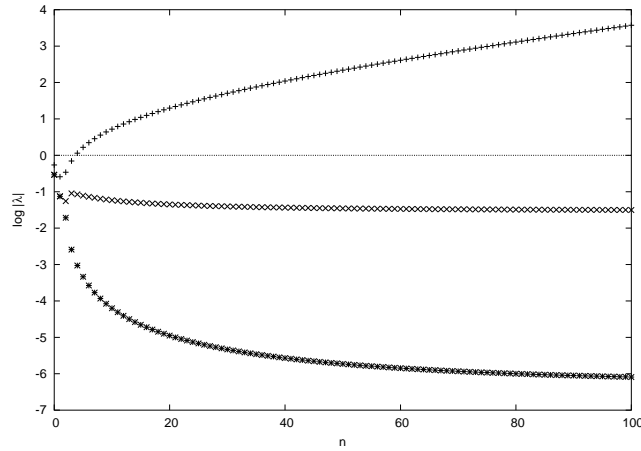
Figure 11. For the parameters $s_1 = 1.0, s_2 = 1.4, s_3 = 0.8$, this graph shows the logarithm of the Floquet multipliers against n, for the map (9). Again, $\alpha_3 < 0$, so for all large n the fixed point is unstable.

4. Irregular cycling

As hinted at earlier, numerical integrations have indicated the possibility of trajectories displaying sustained irregular cycling behaviour, that is, the number of loops around each sub-cycle does not settle down to a constant value but behaves in an irregular way. Figure 10 shows an example of this for four trajectories with $s_1 = 1.0, s_2 = 1.4, s_3 = 0.8$. Notice how the number of loops seems to be 'trapped' in a band between roughly $n = 35$ and $n = 45$. The initial conditions for three of the trajectories were very close together.

The Floquet multipliers for the positive fixed point of the map (9) for these parameter values are shown in figure 11. Since $\alpha_3 < 0$, the fixed points for the range of n covered by the irregular cycling are all unstable. However, there are stable fixed points for $n = 0, 1, 2, 3$, and initial conditions for several trajectories undergoing regular cycling with these values of n have been found numerically. For these parameter values stable regular and irregular cycling coexist.

In the remainder of this section we will state and prove two lemmas for irregular cycling. First, we show that for some parameter values the number of loops around each cycle can be trapped in a band. More precisely:

Lemma 1 *There exists an open region of parameter space, R_T, and for each point in R_T, there exists integers $n_{\min}$, $n_{\max}$ and reals $r_{\min}$, $r_{\max}$, such that if*

$$n_{\min} < n_i < n_{\max}, \text{ and } r_{\min} < r_i < r_{\max}, \text{ for } j - 2 \leq i \leq j$$

for some integer j then

$$n_{\min} < n_i < n_{\max}, \text{ and } r_{\min} < r_i < r_{\max}, \text{ for all } i > j$$

Also, there is an open subset $\hat{R}_T \subset R_T$ where for each $n : n_{\min} < n < n_{\max}$, the positive fixed point of (9) is unstable.

We show also that all periodic sequences of loops are unstable, hence the only possible kind of cycling is necessarily aperiodic and 'irregular'. We suppose that the number of loops around each cycle forms a sequence of integers $\{n_i\}$, and the ratios of the times spent on each cycle forms a sequence of reals $\{r_i\}$. First we define what we mean by periodic cycling.

Definition 4 *A trajectory undergoes k-periodic cycling if the number of loops $\{n_i\}$ around successive sub-cycles is a periodic sequence with period k.*

Recall that the recurrence relation for the ratio sequence $\{r_i\}$ is given by

$$\boldsymbol{r_{i+1}} \equiv \begin{pmatrix} u_{i+1} \\ v_{i+1} \\ r_{i+1} \end{pmatrix} = f_j \begin{pmatrix} u_i \\ v_i \\ r_i \end{pmatrix} = \begin{pmatrix} v_i \\ r_i \\ A_1(n_j) + \frac{A_2(n_{j-1})}{r_i} + \frac{A_3(n_{j-2})}{r_i v_i} + \frac{A_4(n_{j-3})}{r_i u_i v_i} \end{pmatrix} \quad (10)$$

where $j = i \bmod k$. k-periodic cycling trajectories correspond to fixed points of the composition map $F = f_k \circ f_{k-1} \circ ... \circ f_2 \circ f_1$ which implicitly depends on the sequence of numbers of loops $\{n_i\}$. Our second result is:

Lemma 2 *There exists an open region of parameter space, R_U, such that for each point in R_U there exists an integer $N_{\min}$ such that any k-periodic cycling solution trajectory of (2) with sequence $\{n_1, ..., n_k\}$ such that $\min\{n_1, ..., n_k\} \geq N_{\min}$, is unstable as a fixed point of F.*

4.1. Proof of lemma 1

This proof is divided into two parts. We first show that the number of loops around a cycle depends only on two of the co-ordinates of the trajectory as it approaches the cycle. We then use this information inductively to give bounds on the number of loops around subsequent cycles.

4.1.1. Part 1 For simplicity, we consider the trajectory as it begins to approach cycle 1 (the $\xi_2 - \xi_1 - \eta_3$ sub-cycle, see table 2 and figure 2), and we examine the y_1 and x_3 co-ordinates at the point when the trajectory arrives close to the ξ_2 equilibrium from the y_3 direction, setting $y_3 = h$, $y_1 = \tilde{y}_1$, $x_3 = \tilde{x}_3$. (We are again implicitly using the small box approach here.)

From the definition of T_1 as the time spent near ξ_2 we have

$$\tilde{y}_1 e^{s_2 T_1} = h \quad (11)$$

since ξ_2 is unstable in the y_1 direction.

Near ξ_2, the x_3 co-ordinate decays by a factor e^{-cT_1}; in addition after n_1 loops around the $\eta_1 - \eta_3 - \xi_2$ sub-cycle it decays by a further factor $\exp(-s_1 \alpha_3 \Delta_{n_1} T_1)$. This factor can be read off from table 2 because, by symmetry, the growth or decay of x_3 on cycle 1 is equivalent to the growth or decay of x_1 on cycle 3. Finally, x_3 grows by a factor $e^{s_2 T_2}$ whilst near η_1 and is then equal to h. So overall we have

$$\tilde{x}_3 \exp(-cT_1 - s_1 \alpha_3 \Delta_{n_1} + s_2 T_2) \equiv \tilde{x}_3 \exp(-s_2 A_1(n_1) T_1 + s_2 T_2) = h \quad (12)$$

using (7). Rearranging and combining (11) and (12) gives

$$s_2 T_1 = \log\left(\frac{h}{\tilde{y}_1}\right)$$

$$s_2 T_2 = A_1(n_1)\log\left(\frac{h}{\tilde{y}_1}\right) + \ln\left(\frac{h}{\tilde{x}_3}\right)$$

Since the trajectory makes exactly n_1 loops around cycle 1 before switching onto cycle 2, we know that

$$T_2 < T_1 \frac{s_1}{e}\delta^{\star n_1}$$

in order to escape onto cycle 2; the right-hand side is the length of time that the trajectory would have spent on the n_1th pass near η_1 if it were going to complete $n_1 + 1$ loops of cycle 1. Similarly, we also know that

$$\hat{T}_2 > T_1 \frac{s_1}{e}\delta^{\star n_1 - 1}$$

where $\hat{T}_2$ satisfies

$$\tilde{x}_3 \exp(-s_2 A_1(n_1 - 1)T_1 + s_2 \hat{T}_2) = h \tag{13}$$

and is the length of time that would have been spent near η_1 if the trajectory had only completed $n_1 - 1$ loops on cycle 1, before switching to cycle 2.

Hence, substituting for T_1, T_2 and $\hat{T}_2$ in (12) and (13) we find

$$G(n_1 - 1)\log\left(\frac{h}{\tilde{y}_1}\right) < \log\left(\frac{h}{\tilde{x}_3}\right) < G(n_1)\log\left(\frac{h}{\tilde{y}_1}\right) \tag{14}$$

where

$$G(n) = \frac{s_1}{e}\delta^{\star n} - A_1(n)$$

is clearly an increasing function of n when $A_1(n) < 0$ and $\Delta_n > c/(-\alpha_3 s_1)$ (this requires $\alpha_3 < 0$ which we will assume for the remainder of the proof).

When $0 < \tilde{x}_3, \tilde{y}_1 \ll h$ we can ignore the $\log h$ terms in (14), to obtain

$$\tilde{y}_1^{G(n_1)} < \tilde{x}_3 < \tilde{y}_1^{G(n_1 - 1)} \tag{15}$$

Hence the number of loops n_1 on cycle 1 depends only on the y_1 and x_3 co-ordinates as the trajectory approaches ξ_2. Moreover, as $\tilde{y}_1$ and $\tilde{x}_3$ become very small, n_1 depends only on the ratio $\log\tilde{x}_3/\log\tilde{y}_1$.

4.1.2. Part 2 We now use this information about the magnitude of $\tilde{x}_3$ to determine the possible values of n_1, depending on the number of loops around previous cycles (denoted n_0, n_{-1}, n_{-2}). The x_3 co-ordinate was last $\mathcal{O}(1)$ when the trajectory was near ξ_3, and in a similar method to that used to construct table 2, we find that

$$\tilde{x}_3 = h\exp(-s_2 A_2(n_0)T_0 - s_2 A_3(n_{-1})T_{-1} - s_2 A_4(n_{-2})T_{-2}) \tag{16}$$

From (15) we have that

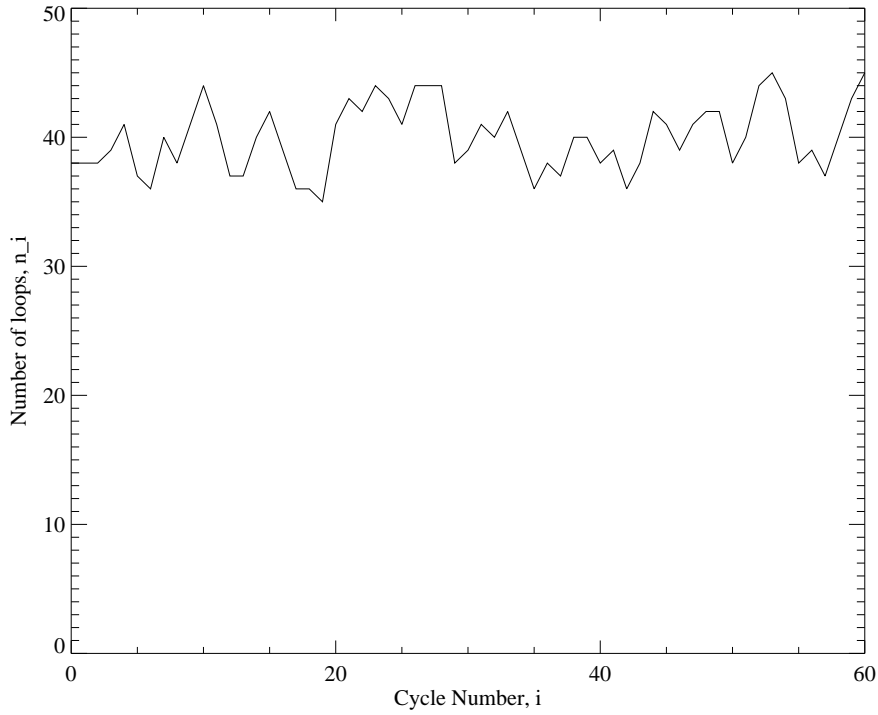$$G(n_1 - 1) < \frac{|\log\tilde{x}_3|}{|\log\tilde{y}_1|} < G(n_1)$$

Figure 12. The graph shows the sequence $\{n_i\}$ as predicted by equations (18) and (19) for parameter values $s_1 = 1.0, s_2 = 1.4, s_3 = 0.8$, and initial conditions $r_1 = r_2 = r_3 = 3.8$ and $n_0 = n_1 = n_2 = 38$. Notice the similarity to figure 10.

and substituting in from (11) and (16), and again ignoring the $\log h$ terms we find

$$G(n_1 - 1) < \frac{A_2(n_0)}{r_1} + \frac{A_3(n_{-1})}{r_1 r_0} + \frac{A_4(n_{-2})}{r_1 r_0 r_{-1}} < G(n_1) \tag{17}$$

or, more generally,

$$G(n_{i+1} - 1) < \frac{A_2(n_i)}{r_{i+1}} + \frac{A_3(n_{i-1})}{r_{i+1} r_i} + \frac{A_4(n_{i-2})}{r_{i+1} r_i r_{i-1}} < G(n_{i+1}) \tag{18}$$

so in the range in which $G(n)$ is strictly increasing this give a unique value for n_{i+1} if we also know r_{i+1}, r_i and r_{i-1}. However, we already have a recurrence relation for the r_i:

$$r_{i+1} = A_1(n_i) + \frac{A_2(n_{i-1})}{r_i} + \frac{A_3(n_{i-2})}{r_i r_{i-1}} + \frac{A_4(n_{i-3})}{r_i r_{i-1} r_{i-2}} \tag{19}$$

Iterating (18) and (19) together with initial conditions n_0, n_1, n_2, and r_1, r_2, r_3 should give the sequences. For parameter values $s_1 = 1.0, s_2 = 1.4, s_3 = 0.8$ this give us very similar results to those seen from integrations, shown in figure 12. However, the results do not agree quantitatively, the main source of error is on the transitions between the sub-cycles: as the transverse component grows the trajectory moves away from the equilibrium and the linearisation becomes less accurate. The analysis is not necessarily more accurate in the large n limit.

We now use (18) and (19) iteratively to show that the sequences $\{n_i\}$ and $\{r_i\}$ can remain bounded within a band. Putting (18) and (19) together gives

$$G(n_i - 1) < r_{i+1} - A_1(n_i) < G(n_i)$$

which simplifies to yield

$$\left(\frac{s_3}{c} + \frac{c}{s_2}\right)\delta^{\star n_i} < r_{i+1} < \frac{s_1}{e}\delta^{\star n_i} \tag{20}$$

so inverting and multiplying by $A_2(n_i)$ we have that

$$\frac{A_2(n_i)}{\frac{s_1}{e}\delta^{\star n_i}} < \frac{A_2(n_i)}{r_{i+1}} < \frac{A_2(n_i)}{\left(\frac{s_3}{c} + \frac{c}{s_2}\right)\delta^{\star n_i}}$$

Recall that for large n, $A_2(n) \sim s_1\gamma_3\Delta_n/s_2$ and notice that

$$\frac{\Delta_n}{\delta^{\star n}} = \frac{\delta^{\star n} - 1}{\delta^{\star n}(\delta^\star - 1)}$$

is an increasing function of n. We now suppose that for cycles i, $i-1$, $i-2$ and $i-3$, $n_{\min} < n_i < n_{\max}$ and $r_{\min} < r_i < r_{\max}$. Then we can assert

$$\frac{A_2(n_{\min})}{\frac{s_1}{e}\delta^{\star n_{\min}}} < \frac{A_2(n_i)}{r_{i+1}} < \frac{A_2(n_{\max})}{\left(\frac{s_3}{c} + \frac{c}{s_2}\right)\delta^{\star n_{\max}}}$$

and similar expressions for A_3 and A_4. Now, using the bounds in (20) and (18) we can guarantee that $n_{\min} < n_{i+1} < n_{\max}$ and $r_{\min} < r_{i+1} < r_{\max}$ if

$$\frac{A_2(n_{\min}) + \frac{A_3(n_{\min})}{r_{\max}} + \frac{A_4(n_{\min})}{r_{\max}^2}}{\frac{s_1}{e}\delta^{\star n_{\min}}} > G(n_{\min}) \tag{21}$$

$$\frac{A_2(n_{\max}) + \frac{A_3(n_{\max})}{r_{\min}} + \frac{A_4(n_{\max})}{r_{\min}^2}}{\left(\frac{s_3}{c} + \frac{c}{s_2}\right)\delta^{\star n_{\max}}} < G(n_{\max} - 1) \tag{22}$$

$$\frac{s_1}{e}\delta^{\star n_{\max}} \qquad\qquad < r_{\max} \tag{23}$$

$$\left(\frac{s_3}{c} + \frac{c}{s_2}\right)\delta^{\star n_{\min}} > r_{\min} \tag{24}$$

These four inequalities define possible sets of bounds $\{n_{\min}, n_{\max}, r_{\min}, r_{\max}\}$. Our task is now to find the best possible set of values. Clearly (21) is not satisfied for very large $n_{\min}$. Setting $r_{\max} = \infty$, and then (for definiteness) find the largest $n_{\min}$ that satisfies (21); this is our initial estimate for $n_{\min}$. If this estimate is negative, then set $n_{\min} = 0$.

Now, using this estimate for $n_{\min}$, we find the largest $r_{\min}$ that satisfies (24). Having found an estimate for $r_{\min}$, we now use (22) to estimate $n_{\max}$ as the smallest value for which (22) holds. From $n_{\max}$ we use (23) to find a smaller estimate for $r_{\max}$; initially we had set $r_{\max} = \infty$. This process can be repeated until convergence is attained. Clearly $n_{\min}$ will increase as we iterate, since the l.h.s. of (21) increases when $r_{\max}$ decreases; similarly $n_{\max}$ will decrease. Therefore, for any parameter sets with $\alpha_3 < 0$

Table 4. The table shows the values obtained when iterating equations (21) to (24) for the parameter values $s_1 = 1.0$, $s_2 = 1.4$, $s_3 = 0.8$.

iteration	$r_{\max}$	$n_{\min}$	$r_{\min}$	$n_{\max}$
1	∞	14	2.009	58
2	6.455	25	2.509	54
3	5.954	26	2.561	54

(and $\beta_3, \gamma_1 < 0$) we will be able to find bounds $n_{\min}$, $n_{\max}$ within which the n_i remain trapped. For a subset of these collections of parameter values, the smallest n for which regular cycling is stable (as discussed in section 3.2.1) will be less than $n_{\min}$, and so trapped trajectories cannot undergo regular cycling. This will occur for those parameters for which (21) is more easily satisfied for larger $n_{\min}$, for example when $e\gamma_3/s_2$ is larger (and hence the l.h.s. of (21) is larger) or when $s_1(-\alpha_3)/s_2$ is smaller (so that the r.h.s. of (21) is smaller). $\qquad\square$

For the parameter values $s_1 = 1.0$, $s_2 = 1.4$, $s_3 = 0.8$, we compute bounds of $n_{\min} = 26$ and $n_{\max} = 54$, which are in good agreement with the numerically observed bounds (see figure 10). This convergence occurred after only three iterations, which we show in table 4. All this analysis depends on taking sufficiently large values of n that the coefficients $A_j(n)$ are monotonically increasing in n: for our typical parameter values this is abundantly the case.

4.2. Proof of lemma 2

Suppose the $\{n_i\}$ form a repeating sequence with period k, say $\{n_1, n_2, ..., n_k\}$. Let $N_{\min} = \min\{n_1, ..., n_k\}$ and $N_{\max} = \max\{n_1, ..., n_k\}$. We are interested in the case where $N_{\min}$ is large, so that $A_1(n), ..., A_4(n)$ are dominated by the Δ_n term, see section 3.2 for definitions.

We consider the recurrence relation (10) for the ratio of times spent on the cycles. The Jacobian matrix for the map $\boldsymbol{r_{i+1}} = f_j(\boldsymbol{r_j})$ has the form

$$f_j' = \begin{pmatrix} 0 & 1 & 0 \\ 0 & 0 & 1 \\ -\frac{A_4(n_{j-3})}{r_i v_i u_i^2} & -\frac{A_3(n_{j-2})}{r_i v_i^2} - \frac{A_4(n_{j-3})}{r_i v_i^2 u_i} & -\frac{A_2(n_{j-1})}{r_i^2} - \frac{A_3(n_{j-2})}{r_i^2 v_i} - \frac{A_4(n_{j-3})}{r_i^2 v_i u_i} \end{pmatrix} \qquad (25)$$

We are interested in finding fixed points of $F = f_k \circ f_{k-1} \circ ... \circ f_2 \circ f_1$ since they may correspond to k-periodic cycling solutions of the system (2). Suppose $\boldsymbol{r_1}$ is a fixed point of F, and

$$\boldsymbol{r_{i+1}} = f_j(\boldsymbol{r_i})$$

then the third components of the $\boldsymbol{r_i}$ form a periodic sequence $\{r_1, ..., r_k\}$. The stability of this fixed point $\boldsymbol{r_1} = F(\boldsymbol{r_1})$ is determined by the eigenvalues of the matrix

$$F'(\boldsymbol{r_1}) = f_k'(\boldsymbol{r_k}) f_{k-1}'(\boldsymbol{r_{k-1}}) ... f_2'(\boldsymbol{r_2}) f_1'(\boldsymbol{r_1}) = \prod_{j=1}^{k} f_j'(\boldsymbol{r_j})$$

If all eigenvalues (Floquet multipliers of the map) have modulus less than 1, the solution is stable, otherwise it is unstable. A fixed point of the map (10) can be interpreted as a cycling cycles solution of equation (2) if $r_j > 0$, $j = 1, ..., k$.

We are able to estimate the largest eigenvalue of $F'(\boldsymbol{r_1})$ through estimates of the largest eigenvalues of the matrices $f_j'(r_j)$ since the eigenvectors all lie close the the $(0, 0, 1)^\top$ direction for the type of fixed point we find we need to analyse.

We now consider the possible types of fixed points of F. First we consider the possibility of a fixed point with all r_j being of order 1 (and $N_{\min}$ is large). Since, in the limit we are considering, $|A_1|, ..., |A_4|$ are large, and we must have all $r_j > 0$, a fixed point is possible only if $A_1 < 0$ and there is cancellation between the large terms in the recurrence relation (10). A solution of this form will have

$$f_j'(\boldsymbol{r_j}) = \begin{pmatrix} 0 & 1 & 0 \\ 0 & 0 & 1 \\ E_{j1} & E_{j2} & E_{j3} \end{pmatrix}$$

where there exist order 1 constants (by which we mean independent of n) $\hat{k}_{jm}$, k_{jm} such that

$$\hat{k}_{jm}\Delta_{N_{\min}} < |E_{jm}| < k_{jm}\Delta_{N_{\max}}$$

Note that in the following we bound quantities above and below but in fact, we can take $N_{\max}$ to be as large as we want here. We use $N_{\max}$ in only one part of the proof, contained in Appendix B; this part of the discussion is slightly tangential since the fixed point it discusses has no physical interpretation in terms of cycling trajectories for the parameter values we consider. Now we will show by induction that for all $k \geq 2$, there are order 1 constants $c_{lm}(k), d_{lm}(k)$ and reals $D_{lm}(k)$ satisfying

$$c_{lm}(k)\Delta_{N_{\min}} < |D_{lm}(k)| < d_{lm}(k)\Delta_{N_{\max}} \tag{26}$$

such that

$$F' \equiv \prod_{j=1}^{k} f_j'(\boldsymbol{r_j}) = \begin{pmatrix} D_{11}(k)^{k-2} & D_{12}(k)^{k-2} & D_{13}(k)^{k-2} \\ D_{21}(k)^{k-1} & D_{22}(k)^{k-1} & D_{23}(k)^{k-1} \\ D_{31}(k)^{k} & D_{32}(k)^{k} & D_{33}(k)^{k} \end{pmatrix} \tag{27}$$

Assuming this is true for $k - 1$, we have

$$\prod_{j=1}^{k} f_j'(\boldsymbol{r_j}) = \begin{pmatrix} 0 & 1 & 0 \\ 0 & 0 & 1 \\ E_{k1} & E_{k2} & E_{k3} \end{pmatrix} \prod_{j=1}^{k-1} f_j'(\boldsymbol{r_j})$$

$$= \begin{pmatrix} 0 & 1 & 0 \\ 0 & 0 & 1 \\ E_{k1} & E_{k2} & E_{k3} \end{pmatrix} \begin{pmatrix} D_{11}(k-1)^{k-3} & D_{12}(k-1)^{k-3} & D_{13}(k-1)^{k-3} \\ D_{21}(k-1)^{k-2} & D_{22}(k-1)^{k-2} & D_{23}(k-1)^{k-2} \\ D_{31}(k-1)^{k-1} & D_{32}(k-1)^{k-1} & D_{33}(k-1)^{k-1} \end{pmatrix}$$

$$= \begin{pmatrix} D_{21}(k-1)^{k-2} & D_{22}(k-1)^{k-2} & D_{23}(k-1)^{k-2} \\ D_{31}(k-1)^{k-1} & D_{32}(k-1)^{k-1} & D_{33}(k-1)^{k-1} \\ D_{31}(k)^{k} & D_{32}(k)^{k} & D_{33}(k)^{k} \end{pmatrix}$$

where for $m = 1, 2, 3$,

$$D_{3m}(k)^k = D_{1m}(k-1)^{k-3}E_{k1} + D_{2m}(k-1)^{k-2}E_{k2} + D_{3m}(k-1)^{k-1}E_{k3}$$

and we can find order 1 constants $c_{3m}(k)$ and $d_{3m}(k)$ so that $D_{3m}(k)$ satisfies the inequality (26). We then define

$$D_{lm}(k) = D_{(l+1)m}(k-1)$$
$$c_{lm}(k) = c_{(l+1)m}(k-1)$$
$$d_{lm}(k) = d_{(l+1)m}(k-1)$$

for $l = 1, 2$ and $m = 1, 2, 3$ to complete the inductive step.

Since

$$f_2'(\mathbf{r_2})f_1'(\mathbf{r_1}) = \begin{pmatrix} 0 & 0 & 1 \\ E_{11} & E_{12} & E_{13} \\ E_{11}E_{23} & E_{21} + E_{12}E_{23} & E_{22} + E_{13}E_{23} \end{pmatrix}$$

$$= \begin{pmatrix} 0 & 0 & 1 \\ E_{11} & E_{12} & E_{13} \\ (D_{31}(2))^2 & (D_{32}(2))^2 & (D_{33}(2))^2 \end{pmatrix}$$

for some order 1 constants $c_{3m}(2)$, $d_{3m}(2)$ chosen so that

$$c_{3m}(2)\Delta_{N_{\min}} < D_{3m}(2) < d_{3m}(2)\Delta_{N_{\max}}$$

then the inductive hypotheses (26) and (27) are true for $k = 2$, and hence for all $k > 2$.

We now want to consider the eigenvalues of the matrix

$$F' = \begin{pmatrix} D_{11}(k)^{k-2} & D_{12}(k)^{k-2} & D_{13}(k)^{k-2} \\ D_{21}(k)^{k-1} & D_{22}(k)^{k-1} & D_{23}(k)^{k-1} \\ D_{31}(k)^{k} & D_{32}(k)^{k} & D_{33}(k)^{k} \end{pmatrix}$$

We can calculate the determinant exactly, because $\det f_j'(\mathbf{r_j}) = E_{j1}$, and it is straight forward to estimate the trace from the matrix above; hence

$$\det F' = c_1 D^k \quad \text{tr} F' = c_2 D^k$$

where $\Delta_{N_{\min}} < D < \Delta_{N_{\max}}$ and c_1, c_2 are (more) order 1 constants. So F' must have exactly one eigenvalue $\lambda = c_3 D^k$ with c_3 order 1. Then for $N_{\min}$ sufficiently large, $|\lambda| > 1$ and solutions with r_j order 1 are unstable.

We next consider the form of other possible fixed points. First suppose there is a k-periodic cycling trajectory with $\{r_1, ..., r_{k-1}\}$ order 1 but r_k large, say $r_k = c\Delta_n$ for some order 1 constant c, and $N_{\min} \leq n \leq N_{\max}$. Then, using (10), we find that $r_1 - A_1(n_k)$ is of order 1, and hence we have a contradiction since r_1 must now be order Δ_{n_k}. In fact, we can try to find solutions with other scalings, i.e. by trying $r_j = c_r D^\beta$, $v_j = c_v D^\gamma$, $u_j = c_u D^\sigma$, for c_i order 1. We can estimate the next terms in the recurrence relation by substituting these scalings into (10), for different combinations of signs of the exponents β, γ, and σ. We find that unless $\beta = \gamma = \sigma = 0$ (the solution type where all the r_j are order 1, considered previously), then we always have that

$\hat{c}_1 \Delta_{N_{\min}} < r_{j+2}, r_{j+3}, r_{j+4} < \hat{c}_2 \Delta_{N_{\max}}$ for some order 1 constants $\hat{c}_1$ and $\hat{c}_2$, and hence all r_j must be large.

The only remaining possibility is that all the r_j are large. We now consider this solution in detail. From equation (7) we see that for Δ_n large, we have

$$A_1(n) \sim \frac{s_1}{s_2}\alpha_3\Delta_n \qquad A_2(n) \sim \frac{s_1}{s_2}\gamma_3\Delta_n$$

$$A_3(n) \sim \frac{s_1}{s_2}\beta_3\Delta_n \qquad A_4(n) = \frac{s_1}{s_2}\delta^{\star n} \sim \frac{s_1(\delta^\star - 1)}{s_2}\Delta_n$$

From (10) we can approximate r_{j+1} by

$$r_{j+1} \approx A_1(n_j) + \frac{A_2(n_{j-1})}{A_1(n_{j-1})}$$

moreover, we can find order 1 constants $\tilde{c}_1$ and $\tilde{c}_2$ such that

$$\tilde{c}_1\hat{\varepsilon} < \left| r_{j+1} - \left(A_1(n_j) + \frac{A_2(n_{j-1})}{A_1(n_{j-1})} \right) \right| < \tilde{c}_2\varepsilon$$

where we define

$$\varepsilon = \max_{n_i \in \{n_1,\dots,n_k\}} \left\{ \frac{A_2(n_i)}{A_1(n_i)^2}, \frac{A_3(n_{i-1})}{A_1(n_i)A_1(n_{i-1})}, \frac{A_4(n_{i-1})}{A_1(n_i)A_1(n_{i-1})}, \frac{1}{|A_1(n_i)|} \right\}$$

$$= \max \left\{ \frac{A_2(N_{\min})}{A_1(N_{\min})^2}, \frac{A_3(N_{\min})}{A_1(N_{\min})^2}, \frac{A_4(N_{\min})}{A_1(N_{\min})^2}, \frac{1}{|A_1(N_{\min})|} \right\}$$

$$= \frac{e_1}{\Delta_{N_{\min}}}$$

for some order 1 constant e_1, assuming $N_{\min}$ is large enough that $|A_1(n)|$ is an increasing function of n for $n > N_{\min}$, and $|A_2(n)/A_1(n)|$ tends to a constant as $n \to \infty$ (as does $|A_3(n)/A_1(n)|$ and $|A_4(n)/A_1(n)|$). Similarly we define

$$\hat{\varepsilon} = \min_{n_i \in \{n_1,\dots,n_k\}} \left\{ \frac{A_2(n_i)}{A_1(n_i)^2}, \frac{A_3(n_{i-1})}{A_1(n_i)A_1(n_{i-1})}, \frac{A_4(n_{i-1})}{A_1(n_i)A_1(n_{i-1})}, \frac{1}{|A_1(n_i)|} \right\}$$

$$= \min \left\{ \frac{A_2(N_{\max})}{A_1(N_{\max})^2}, \frac{A_3(N_{\max})}{A_1(N_{\max})^2}, \frac{A_4(N_{\max})}{A_1(N_{\max})^2}, \frac{1}{|A_1(N_{\max})|} \right\}$$

$$= \frac{e_2}{\Delta_{N_{\max}}}$$

for some order 1 constant e_2.

Appendix B shows that for a given $N_{\min}$, we can find an $N_{\max}$ the map (10) has a stable fixed point with all the $|r_j|$ large regardless of the sign of A_1. However, in the case $A_1 < 0$ this fixed point will not be relevant to the behaviour of solution trajectories to the system (2) because at least some of the r_j will be negative. This is the only part of the proof to use the upper bound $N_{\max}$.

Therefore if $\alpha_3 < 0$ then we can find an $N_{\min}$ such that $A_1(n) < 0$ for $n > N_{\min}$ and the only relevant fixed points for the map F are those with all r_j of order 1 and these are unstable so long as $\Delta_{N_{\min}}$ is large enough. Hence there can be no stable k-periodic cycling solutions. $\qquad\square$

Remark If $A_1 > 0$, then the k-periodic cycling solutions can be stable, but also all

regular (1-periodic) cycling solutions are stable. Numerical simulations have shown trajectories converging to the regular cycling solutions where n is constant, but it may be possible to find initial conditions for trajectories which display k-periodic cycling behaviour for $k > 1$.

Remark The open sets $\hat{R}_T$ and R_U have a non-empty intersection, and moreover, there is a subset of the intersection for which $N_{\min} < n_{\min}$.

To justify this remark we observe that the parameter values $s_1 = 1.0$, $s_2 = 1.4$, $s_3 = 0.8$ are contained in both $\hat{R}_T$ and R_U, with $n_{\min} = 26$, and $n_{\max} = 53$. Taking $N_{\min} = 25$ gives a sufficiently large $\Delta_{N_{\min}}$ for lemma 2 to hold, and hence all trajectories are trapped in a region where there are no periodic solutions, and hence must display irregular cycling behaviour.

5. Conclusions

In this paper we have examined a structurally stable heteroclinic network in $\mathbb{R}^6$, with symmetry $\mathbb{Z}_3 \ltimes \mathbb{Z}_2^6$. The system contains a number of parameters which can be varied in order to find different types of behaviour. We have shown that there is a subset of parameter values for which none of the sub-cycles in the network can be e.a.s., but the network as a whole is still strongly attracting. In this particular case, the network resembles three copies of the system studied by Kirk and Silber (1994).

To simplify the calculations we then enlarged the symmetry group to $\mathbb{Z}_6 \ltimes \mathbb{Z}_2^6$, so the network contained six symmetric sub-cycles, and concentrated on a particular type of trajectory which occurs when each sub-cycle is unstable in one transverse direction. In this case switching between neighbourhoods of the sub-cycles can occur in a cyclical manner. We demonstrated analytically that this 'cycling cycles' behaviour can be regular or irregular, depending on both parameter values and the initial conditions of the trajectory.

An interesting question to ask about the irregular cycling is whether in some sense the trajectories can be thought of as chaotic. Numerical simulations have indicated the presence of 'sensitive dependence on initial conditions'. Clearly the orbits in $\mathbb{R}^6$ are not dense, because the trajectories are always converging to the heteroclinic network.

Our analysis gives rise to many questions concerning the dynamics near heteroclinic networks; for example is this combination of regular and irregular behaviour typical for networks with a particular structure, and to what extent is it possible to characterise the possibilities in terms of the underlying equivariance of the vector field?

There are a number of ways in which our specific vector field could be generalised. For example we could form an analogous sequence of $2n$ 3-cycles by coupling together a pair of cycles similar to the two Guckenheimer–Holmes 3-cycles in the $\boldsymbol{x}$ and $\boldsymbol{y}$-subspaces but containing $n > 3$ equilibria. Such a vector field in $\mathbb{R}^{2n}$ would naturally be $\mathbb{Z}_{2n} \ltimes \mathbb{Z}_2^{2n}$-symmetric. It seems very likely that similar regular and irregular cycling behaviour would occur in this situation. More interestingly, we could aim to construct lower-

dimensional examples of these dynamics, hopefully exploiting the complete classification of homoclinic cycles in $\mathbb{R}^4$ given recently by Sottocornola (2003). Alternatively, we could investigate vector fields in $\mathbb{R}^6$ that are equivariant under different symmetry groups; the behaviour described here may exist only for 'sufficiently complicated' group actions. In the present system, the cycling occurs between cycles which are of type B (in the 'A,B,C classification' of Chossat *et al* (1997)).

Of more physical relevance would be study of the effects of introducing small symmetry-breaking terms, for example quadratic terms. Such perturbations would break some, but crucially not all, of the heteroclinic connecting orbits and may generate periodic orbits in their place. Work on some of these problems is ongoing.

Acknowledgments

Appendix A.

In this appendix we give the details of the calculations of the results in section 2.4. Recall that:

$$\hat{\delta}_x = \frac{t_2}{t_3} \qquad \hat{\delta}_y = \frac{s_1}{s_2} \qquad \delta_2 = \frac{c}{s_2} \qquad \delta_3 = \frac{s_1}{e} \qquad \tilde{\delta}_1 = \frac{c}{t_3} \qquad \tilde{\delta}_2 = \frac{t_2}{e}$$

Also, recall the exponents for the yyx-cycle are:

$$\alpha_1 = \frac{c}{t_3} - \frac{s_2}{e}\hat{\delta}_x + \frac{s_3}{s_2}\hat{\delta}_x\delta_3 \qquad \beta_1 = -\frac{e}{t_3} + \frac{s_3}{e}\hat{\delta}_x + \frac{s_1}{s_2}\hat{\delta}_x\delta_3 \qquad \gamma_1 = \frac{t_1}{t_3} + \frac{c}{e}\hat{\delta}_x - \frac{e}{s_2}\hat{\delta}_x\delta_3$$

$$\alpha_2 = \frac{s_3}{s_2} + \frac{c}{t_3}\delta_2 - \frac{s_2}{e}\delta_2\hat{\delta}_x \qquad \beta_2 = \frac{s_1}{s_2} - \frac{e}{t_3}\delta_2 + \frac{s_3}{e}\delta_2\hat{\delta}_x \qquad \gamma_2 = -\frac{e}{s_2} + \frac{t_1}{t_3}\delta_2 + \frac{c}{e}\delta_2\hat{\delta}_x$$

$$\alpha_3 = -\frac{s_2}{e} + \frac{s_3}{s_2}\delta_3 + \frac{c}{t_3}\delta_2\delta_3 \qquad \beta_3 = \frac{s_3}{e} + \frac{s_1}{s_2}\delta_3 - \frac{e}{t_3}\delta_2\delta_3 \qquad \gamma_3 = \frac{c}{e} - \frac{e}{s_2}\delta_3 + \frac{t_1}{t_3}\delta_2\delta_3$$

Simple manipulations give the following relations:

$$\hat{\delta}_x\alpha_3 = \frac{c}{t_3}(\delta^\star - 1) + \alpha_1$$

$$\delta_2\alpha_1 = \frac{s_3}{s_2}(\delta^\star - 1) + \alpha_2$$

$$\delta_2\beta_1 = \frac{s_1}{s_2}(\delta^\star - 1) + \beta_2$$

$$\delta_3\beta_2 = \frac{s_3}{e}(\delta^\star - 1) + \beta_3$$

$$\delta_3\gamma_2 = \frac{c}{e}(\delta^\star - 1) + \gamma_3$$

$$\hat{\delta}_x\gamma_3 = \frac{t_1}{t_3}(\delta^\star - 1) + \gamma_1$$

and so if $\delta^\star > 1$ it is clear that

$$\alpha_2 > 0 \Rightarrow \alpha_1, \alpha_3 > 0$$
$$\beta_3 > 0 \Rightarrow \beta_1, \beta_2 > 0$$
$$\gamma_1 > 0 \Rightarrow \gamma_2, \gamma_3 > 0$$

The equivalent exponents for the xxy-cycle are:

$$\tilde\alpha_1 = -\frac{e}{t_3} + \frac{s_3}{s_2}\tilde\delta_1 + \frac{c}{e}\tilde\delta_1\hat\delta_y \qquad \tilde\beta_1 = \frac{t_1}{t_3} + \frac{c}{s_2}\tilde\delta_1 - \frac{t_3}{e}\tilde\delta_1\hat\delta_y \qquad \tilde\gamma_1 = \frac{t_2}{t_3} - \frac{e}{s_2}\tilde\delta_1 - \frac{t_1}{e}\tilde\delta_1\hat\delta_y$$

$$\tilde\alpha_2 = \frac{c}{e} - \frac{e}{t_3}\tilde\delta_2 + \frac{s_3}{s_2}\tilde\delta_2\tilde\delta_1 \qquad \tilde\beta_2 = -\frac{t_3}{e} + \frac{t_1}{t_3}\tilde\delta_2 + \frac{c}{s_2}\tilde\delta_2\tilde\delta_1 \qquad \tilde\gamma_2 = \frac{t_1}{e} + \frac{t_2}{t_3}\tilde\delta_2 - \frac{e}{s_2}\tilde\delta_2\tilde\delta_1$$

$$\tilde\alpha_3 = \frac{s_3}{s_2} + \frac{c}{e}\hat\delta_y - \frac{e}{t_3}\tilde\delta_2\hat\delta_y \qquad \tilde\beta_3 = \frac{c}{s_2} - \frac{t_3}{e}\hat\delta_y + \frac{t_1}{t_3}\tilde\delta_2\hat\delta_y \qquad \tilde\gamma_3 = -\frac{e}{s_2} + \frac{t_1}{e}\hat\delta_y + \frac{t_2}{t_3}\hat\delta_y\tilde\delta_2$$

and similar relations between these coefficients can be found:

$$\tilde\delta_2\tilde\alpha_1 = \frac{c}{e}(\delta^\star - 1) + \tilde\alpha_2$$

$$\hat\delta_y\tilde\alpha_2 = \frac{s_3}{s_2}(\delta^\star - 1) + \tilde\alpha_3$$

$$\hat\delta_y\tilde\beta_2 = \frac{c}{s_2}(\delta^\star - 1) + \tilde\beta_3$$

$$\tilde\delta_1\tilde\beta_3 = \frac{t_1}{t_3}(\delta^\star - 1) + \tilde\beta_1$$

$$\tilde\delta_2\tilde\gamma_1 = \frac{t_1}{e}(\delta^\star - 1) + \tilde\gamma_2$$

$$\tilde\delta_1\tilde\gamma_3 = \frac{t_2}{t_3}(\delta^\star - 1) + \tilde\gamma_1$$

meaning that:

$$\tilde\alpha_3 > 0 \Rightarrow \tilde\alpha_1, \tilde\alpha_2 > 0$$
$$\tilde\beta_1 > 0 \Rightarrow \tilde\beta_2, \tilde\beta_3 > 0$$
$$\tilde\gamma_2 > 0 \Rightarrow \tilde\gamma_1, \tilde\gamma_3 > 0$$

Appendix B.

Here we show that the map $F = f_k \circ f_{k-1} \circ ... \circ f_2 \circ f_1$ has a stable fixed point with $\{r_1, ..., r_k\}$ large. Recall from section 4.2 that we have

$$c_1\hat\varepsilon < \left| r_{j+1} - \left(A_1(n_j) + \frac{A_2(n_{j-1})}{A_1(n_{j-1})} \right) \right| < c_2\varepsilon$$

which implies also that there exist constants c_3, c_4 of order 1 (i.e. independent of n) such that:

$$c_3\varepsilon\hat\varepsilon < \left| \frac{1}{r_{j+1}} - \frac{1}{A_1(n_j)} \right| < c_4\varepsilon\hat\varepsilon$$

Then, defining ϵ_j, δ_j and a_j with reference to (25), viz:

$$f'_j = \begin{pmatrix} 0 & 1 & 0 \\ 0 & 0 & 1 \\ \epsilon_j & \delta_j & a_j \end{pmatrix} = a_i \begin{pmatrix} 0 & \frac{1}{a_j} & 0 \\ 0 & 0 & \frac{1}{a_j} \\ \frac{\epsilon_j}{a_j} & \frac{\delta_j}{a_j} & 1 \end{pmatrix}$$

we find that there are order 1 constants $\hat{c}_i$ such that

$$\hat{c}_1 \hat{\varepsilon}^3 < |\epsilon_i| < \hat{c}_2 \varepsilon^3$$
$$\hat{c}_3 \hat{\varepsilon}^2 < |\delta_i| < \hat{c}_4 \varepsilon^2 \qquad\qquad (\text{B.1})$$
$$\hat{c}_5 \hat{\varepsilon} < |a_i| < \hat{c}_6 \varepsilon$$

and so there are order 1 constants $\tilde{c}_i$ such that

$$\frac{\tilde{c}_1}{\varepsilon} < \frac{1}{|a_i|} < \frac{\tilde{c}_2}{\hat{\varepsilon}}$$
$$\frac{\tilde{c}_3 \hat{\varepsilon}^2}{\varepsilon} < \frac{1}{|\delta_i|} < \frac{\tilde{c}_4 \varepsilon^2}{\hat{\varepsilon}}$$
$$\frac{\tilde{c}_5 \hat{\varepsilon}^3}{\varepsilon} < \frac{1}{|\epsilon_i|} < \frac{\tilde{c}_6 \varepsilon^3}{\hat{\varepsilon}}$$

This tells us that we can write f'_j in the form

$$f'_j = B_j \begin{pmatrix} 1 & 0 & 0 \\ 0 & \varepsilon & 0 \\ 0 & 0 & \varepsilon^2 \end{pmatrix} \begin{pmatrix} 0 & b_1 & 0 \\ 0 & 0 & b_2 \\ b_3 & b_4 & b_5 \end{pmatrix} \begin{pmatrix} 1 & 0 & 0 \\ 0 & \varepsilon^{-1} & 0 \\ 0 & 0 & \varepsilon^{-2} \end{pmatrix}$$

where

$$|B_j| < |a_i| \frac{\varepsilon}{\hat{\varepsilon}}$$

and the b_i are order 1. Also,

$$f'_j = C_j \begin{pmatrix} 1 & 0 & 0 \\ 0 & \hat{\varepsilon} & 0 \\ 0 & 0 & \hat{\varepsilon}^2 \end{pmatrix} \begin{pmatrix} 0 & c_1 & 0 \\ 0 & 0 & c_2 \\ c_3 & c_4 & c_5 \end{pmatrix} \begin{pmatrix} 1 & 0 & 0 \\ 0 & \hat{\varepsilon}^{-1} & 0 \\ 0 & 0 & \hat{\varepsilon}^{-2} \end{pmatrix}$$

where

$$|C_j| > |a_i| \frac{\hat{\varepsilon}}{\varepsilon}$$

and the c_i are order 1. When we calculate $F' \equiv \prod_{j=1}^{k} f'_j$ we find that the matrix product

$$F' \equiv \prod_{j=1}^{k} B_j \begin{pmatrix} 1 & 0 & 0 \\ 0 & \varepsilon & 0 \\ 0 & 0 & \varepsilon^2 \end{pmatrix} M \begin{pmatrix} 1 & 0 & 0 \\ 0 & \varepsilon^{-1} & 0 \\ 0 & 0 & \varepsilon^{-2} \end{pmatrix}$$

$$\equiv \prod_{j=1}^{k} C_j \begin{pmatrix} 1 & 0 & 0 \\ 0 & \hat{\varepsilon} & 0 \\ 0 & 0 & \hat{\varepsilon}^2 \end{pmatrix} \hat{M} \begin{pmatrix} 1 & 0 & 0 \\ 0 & \hat{\varepsilon}^{-1} & 0 \\ 0 & 0 & \hat{\varepsilon}^{-2} \end{pmatrix}$$

where M and $\hat{M}$ are 3×3 matrices with have order 1 entries. Thus M and $\hat{M}$ have order 1 eigenvalues. This tells us that the eigenvalues λ of F' must satisfy

$$K_1 \left(\frac{\hat{\varepsilon}}{\varepsilon} \right)^k \prod_{j=1}^{k} a_j < |\lambda| < K_2 \left(\frac{\varepsilon}{\hat{\varepsilon}} \right)^k \prod_{j=1}^{k} a_j$$

for some order 1 constants K_1 and K_2. Hence, using (B.1), we find

$$|\lambda| < K_3 \left(\frac{\varepsilon^2}{\hat{\varepsilon}} \right)^k$$

which can be ensured to be less than 1 so long as $\varepsilon^2 < \hat{\varepsilon}$ (choosing $N_{\min}$ sufficiently large, or $N_{\max}$ sufficiently small). Hence this fixed point has eigenvalues with modulus less than 1 and is therefore stable.

References

Ashwin P and Field M 1999 Heteroclinic networks in coupled cell systems *Arch Rat. Mech. Anal.* **148** 107-143

Brannath W 1994 Heteroclinic networks on the tetrahedron *Nonlinearity* **7** 1367-1384

Busse F M and Heikes K E 1980 Convection in a rotating layer: A simple case of turbulence *Science* **208** 173-175

Chossat P, Krupa M, Melbourne I and Scheel A (1997) Transverse bifurcations of homoclinic cycles *Physica D* **100** 85-100

Guckenheimer J and Holmes P 1988 Structurally stable heteroclinic cycles *Math. Proc. Camb. Phil. Soc.* **103** 189-192

Hofbauer J and Sigmund K (1988) *The Theory of Evolution and Dynamical Systems* (Cambridge University Press)

Kirk V and Silber M A 1994 Competition between heteroclinic cycles *Nonlinearity* **7** 1605-1621

Krupa M 1997 Robust heteroclinic cycles *J. Nonlinear Sci.* **7** 129-176

Krupa M and Melbourne I 1995 Asymptotic stability of heteroclinic cycles in systems with symmetry *Ergod. Th. & Dynam. Sys.* 121-147

Krupa M and Melbourne I 2002 Asymptotic stability of heteroclinic cycles in systems with symmetry, II *Preprint*

Küppers G and Lortz D 1969 Transition from laminar convection to thermal turbulence in a rotating fluid layer *J. Fluid Mech.* **35** 609-620

Melbourne I 1991 An example of a non-asymptotically stable attractor *Nonlinearity* **4** 835-844

Milnor J 1985 On the concept of attractor *Commun. Math. Phys.* **99** 177-195

Proctor M R E and Jones C A 1988 The interaction of two spatially resonant patterns in thermal convection. Part 1. Exact 1:2 resonance. *J. Fluid. Mech* **188** 301-355

Sottocornola N 2003 Robust homoclinic cycles in $\mathbb{R}^4$ *Nonlinearity* **16** 1-24